

NASA Technical Memorandum 101354

# Nuclear Propulsion—A Vital Technology for the Exploration of Mars and the Planets Beyond

(NASA-TM-101354) NUCLEAR PROPULSION: A  
VITAL TECHNOLOGY FOR THE EXPLORATION OF MARS  
AND THE PLANETS BEYOND (NASA) 47 PCSC 21F

N89-10944

Unclas  
G3/20 0169988

Stanley K. Borowski  
*Lewis Research Center*  
*Cleveland, Ohio*

Prepared for  
Case for Mars III  
cosponsored by the American Astronautical Society, Jet Propulsion Laboratory,  
Los Alamos Laboratory, Ames Research Center, Lyndon B. Johnson Space  
Center, George C. Marshall Space Flight Center, and the Planetary Society  
Boulder, Colorado, July 18-22, 1987

**NASA**



# Nuclear Propulsion - A Vital Technology for the Exploration of Mars and the Planets Beyond

Stanley K. Borowski\*

The physics and technology issues, and performance potential of various direct thrust fission and fusion propulsion concepts are examined. Next to chemical propulsion the solid core fission thermal rocket (SCR) is the only other concept to be experimentally tested at the power (~1.5 - 5.0 GW) and thrust levels (~0.33 - 1.11 MN) required for manned Mars missions. With a specific impulse of ~850 s, the SCR can perform various near-Earth, cislunar and interplanetary missions with lower mass and cost requirements than its chemical counterpart. Beyond the SCR, a succession of advanced nuclear engines can be developed each having improved performance. The gas core fission thermal rocket, with a specific power and impulse of ~50 kW/kg and 5000 s, offers the potential for quick courier trips to Mars (of ~80 days) or longer duration exploration / cargo missions (lasting ~280 days) with starting masses of ~1000 metric tons. Convenient transportation to the outer Solar System will require the development of magnetic and inertial fusion rockets (IFRs). Possessing specific powers and impulses of ~100 kW/kg and 200-300 kiloseconds, IFRs will usher in the era of the true Solar System class spaceship. Even Pluto will be accessible with roundtrip times of less than 2 years and starting masses of ~1500 metric tons.

## INTRODUCTION

The National Aeronautics and Space Administration (NASA) has been considering the manned exploration of Mars since the spring of 1962 when the Future Projects Office of the Marshall Space Flight Center initiated studies of possible Mars missions (Ref. 1). Predating

---

\*Dr. Borowski is a Nuclear Propulsion Analyst and staff member in NASA/Lewis Research Center's Advanced Space Analysis Office, 21000 Brookpark Road, Cleveland, Ohio 44135.

this activity and NASA itself was Project Rover (Ref. 2), a nuclear rocket development program begun in 1955 at Los Alamos Scientific Laboratory (LASL) under the sponsorship of the Atomic Energy Commission (AEC) and the U.S. Air Force. Los Alamos built and tested several hydrogen-cooled, graphite-core reactors early in the Rover program. The encouraging results from the proof-of-principle Kiwi-A reactor series led the newly formed NASA to consider using nuclear thermal rockets for its more difficult space missions which included extended lunar-exploration missions, lunar-base operations and manned planetary exploration.

A joint AEC/NASA Space Nuclear Propulsion Office (SNPO) was established in 1960 to pursue the development of a "Nuclear Engine for Rocket Vehicle Application". The NERVA program had as its objective the development of a flight engine that could provide twice the specific impulse of the best chemical rockets. Both the NERVA technology program and LASL's Rover program were highly successful. Included among their many achievements were demonstrations of engine burn endurance (60 min. at 1100 megawatts (MW) by the NRX-A6 reactor), high power operation (the Phoebus-2A reactor had a design power rating of 5000 MW), and reusability (the eXperimental flight Engine Prototype, the XE-P system, was successfully started 24 times). Despite these accomplishments, work on the second phase of the NERVA program - the development of a flight-rated nuclear engine - was never realized due to changing national priorities that led to the eventual termination of the Rover/NERVA programs in January of 1973.

During this same time period, research on the rotating particle bed (Ref. 3) and gaseous fuel core fission reactor concepts (Ref. 4) was also being conducted. In addition to fission systems, propulsion studies based on the use of nuclear fusion reactions between light isotopes of hydrogen and helium began to appear in the literature (Refs. 5,6) in the 1960's and 1970's.

Today, NASA's vision is again focused on the exploration and colonization of Mars. Convenient transportation of personnel and cargo needed to support colonization activities will require the development of propulsion concepts that are significantly more advanced than our present-day systems. Because the thrust-to-engine weight ratio  $[F(\text{kg})/M_w(\text{kg}) = 2000 \alpha (\text{kW/kg})/g^2 \text{Isp}(\text{s})]$  of a spacecraft is directly proportional to the engine specific power ( $\alpha = P_{\text{jet}}/M_w$ ), large values of  $\alpha$  are required to provide the necessary  $P_{\text{acceleration}}$  levels for rapid interplanetary travel. The high performance rockets of the 21st century will operate for prolonged periods of time while simultaneously demonstrating high jet power ( $P_{\text{jet}}$ ), specific impulse (Isp), and thrust capabilities (see Fig. 1).

Classical chemical (C) propulsion systems are characterized by low mass engines ( $M_w$ ) and attractive values of specific power ( $\alpha \sim 1550$  kW/kg for the SSME engines) but the power per unit mass of ejected matter is small (i.e. low Isp) and great quantities of propellant are needed to essentially push propellant around. Electric propulsion

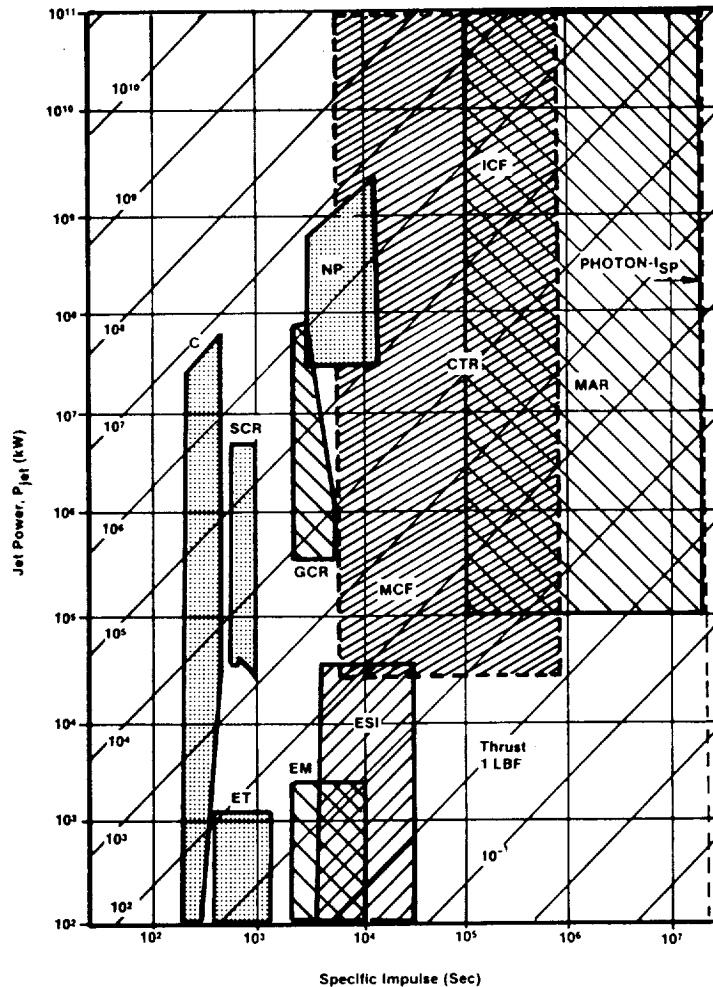


FIGURE 1. - NUCLEAR PROPULSION SYSTEMS CAN PROVIDE THE POWER REQUIREMENTS FOR PRO-  
LONGED HIGH THRUST/HIGH SPECIFIC IMPULSE OPERATION.

(EP) systems use power from an onboard source, such as a nuclear reactor, to accelerate propellant to high exhaust velocities (Isp ~ 1,000 - 10,000 s). However, the added weight of the power conversion and heat rejection systems and the efficiency toll of multiple energy conversion processes result in a low specific power (~0.1 kW/kg) and restrict EP systems to low thrust operation. The pacing element of electric propulsion - the primary power system - is also subject to stringent requirements involving low specific weight and long operating lifetimes (~10,000-20,000 hrs). This last requirement causes concern about the ability to develop these systems to a demonstrated state of reliability before committing them to costly space-flight tests and certainly before committing them to long duration space missions. While additional thrusters can be added to improve reliability of the propulsion system, in the primary power system, such redundancy may add so much weight that EP can lose much of its potential performance margin. However, assuming a favorable

resolution to these problems, the high payload mass fraction capability of EP can be exploited for deep interplanetary or cargo transport missions where long trip times are acceptable.

Direct thrust nuclear propulsion systems based on increasingly more sophisticated forms of nuclear energy conversion involving fission, fusion and mass annihilation (Table 1) provide the means of accessing the attractive high thrust/high Isp area of parameter space shown in Fig. 1. Solid core fission thermal rockets (SCR) developed during the Rover/NERVA program use the thermal energy released in the fission process to heat a working fluid (typically hydrogen), which is then exhausted to provide propulsive thrust. The SCR has a specific impulse capability comparable to the electrothermal (ET) thruster (~800-1000 s) yet delivers thrust levels equivalent to those of chemical engines (~ $10^5$  lbf). The specific power of the SCR is also ~1,000 times larger than that of the ET system.

Table 1  
Yield From Various Energy Sources

<u>Fuels</u>	<u>Reaction Products</u>	<u>Energy Release (J/kg)</u> ( $E/m_i = \Delta c^2$ )	<u>Converted Mass Fraction</u> ( $\alpha = \frac{\Delta m}{m_i} = \frac{m_i - m_f}{m_i}$ )
<u>Chemical</u>			
Conventional: (LO <sub>2</sub> /LH <sub>2</sub> ) Exotics: Atomic Hydrogen Metastable Helium	Water, Hydrogen, Common Helium (He <sup>4</sup> )	1.35x10 <sup>7</sup> 2.18x10 <sup>8</sup> 4.77x10 <sup>8</sup>	1.5x10 <sup>-10</sup> 2.4x10 <sup>-9</sup> 5.3x10 <sup>-9</sup>
<u>Nuclear Fission</u>			
U <sup>233</sup> , U <sup>235</sup> , Pu <sup>239</sup> (~200MeV/U <sup>235</sup> fission)	Radioactive Fission Fragments, Neutrons, γ-Rays	8.2x10 <sup>13</sup>	9.1x10 <sup>-4</sup>
<u>Nuclear Fusion*</u>			
DT (0.4/0.6)	Helium, Neutrons	3.38x10 <sup>14</sup>	3.75x10 <sup>-3</sup>
CAT-DD <sup>†</sup> (1.0)	Hydrogen, Helium & Neutrons	3.45x10 <sup>14</sup>	3.84x10 <sup>-3</sup>
DHe <sup>3</sup> (0.4/0.6)	Hydrogen, Helium (Some Neutrons)	3.52x10 <sup>14</sup>	3.9x10 <sup>-3</sup>
pB <sup>11</sup> (0.1/0.9)	Helium (Thermonuclear Fission)	7.32x10 <sup>13</sup>	8.1x10 <sup>-4</sup>
<u>Matter Plus Antimatter</u>			
p̄p (0.5/0.5)	Annihilation Radiation  Pions Muons Electrons Positrons } Neutrinos & γ-Rays	9x10 <sup>16</sup>	1.0

\* Weight Composition Corresponds to a 50/50 Fusion Fuel Mixture

† CAT-DD - "Catalyzed" DD Reaction Enhanced By Burnup of Reaction Tritons (T) and Helium-3 (He<sup>3</sup>) Nuclei with Deuterons (D) in situ

Notation: U<sup>233</sup>, U<sup>235</sup>, Pu<sup>239</sup> - Fissile Isotopes of Uranium and Plutonium

Δm - Change in Mass Between Reactants (m<sub>i</sub>) and Products (m<sub>f</sub>)

B<sup>11</sup> - Fusionable Isotope of Boron

p, p̄ - Proton and Antiproton

The performance of the SCR is limited, however, by the melting temperature of the fuel, moderator, and core structural materials. By operating the fuel in a high-temperature fissioning plasma state, the gaseous core thermal rocket (GCR) can exhaust propellant at substantially higher values of specific impulse (in the range of electromagnetic (EM) and electrostatic ion (ESI) thrusters, ~3000 to 6000 s) while also demonstrating attractive values of specific power ( $\alpha \sim 10$ -50 kW/kg). Still higher values of Isp (~5000 s to  $10^6$  s) are possible with controlled thermonuclear fusion rockets (CTR). Fusion systems based on magnetic (MCF) and inertial confinement fusion (ICF) can "bridge the gap" between fission systems (examples of which are the nuclear-electric, - thermal and - pulsed (NP) Orion-type concepts shown in Fig. 1), and the relativistic mass annihilation rocket (MAR) of the more distant future.

Direct thrust nuclear propulsion is currently receiving increased attention by both NASA and the Air Force. Under its "Project Forecast II" Study (Ref. 7), the Air Force has identified the fission thermal rocket as a system worthy of development and capable of relatively near term implementation (by the mid 1990's) due to the sizeable technology base that already exists. Air Force sponsored studies (Ref. 8) of direct nuclear orbit transfer vehicles (NOTVs) based on the particle bed reactor concept have shown payload mass fractions of ~50% on one-way missions from low Earth orbit (LEO) to geosynchronous orbit (GEO). Transit times are also short - hours, as compared to months for nuclear electric propulsion (NEP) systems. Even on round trip missions, the NOTV is capable of delivering ~75% more payload to GEO than an expendable  $LO_2/LH_2$  Centaur G. Such performance potential can provide a significant cost savings to the Air Force on its proposed future missions.

For the high payload, high  $\Delta V$  missions currently being studied by NASA, high thrust/high Isp nuclear propulsion systems are expected to provide even greater benefits. These benefits can include either a reduction in the initial mass in Earth orbit (IMEO) and therefore the cost of the mission, or the overall mission trip time. Because of the low specific impulse ( $\sim 450$ s) of today's chemical rockets, NASA's ability to embark on an ambitious program of manned planetary exploration will require the evolutionary development and implementation of increasingly more fuel efficient, and safe, nuclear propulsion systems. The purpose of this paper is to review for the lay person and the professional alike the physics and technology issues associated with various fission and fusion propulsion concepts, and also to compare their performance potential for manned Mars missions in terms of IMEO, payload and propellant mass fractions, and "quick trip" capability. Also summarized briefly are the accomplishments of the Rover/NERVA program and the status of gas core and fusion experimental research.

#### NUCLEAR FUEL CYCLES

An analysis of the yield from various energy sources (Table 1) indicates that only the nuclear fuels (fission, fusion and synthetic antihydrogen fuels) can provide the power requirements for tomorrow's high thrust/high Isp space drives. In addition to energy content, a fuel's reactivity, portability, availability and practicality (charged

particle output in the case of fusion systems) are also important considerations. A large energy yield per reaction or per kilogram of fuel is valuable only if it can be effectively used for propulsive thrust. Synthetic antihydrogen fuel (consisting of an antiproton and a positron) has a specific energy ~ 1,000 times that of fission and ~ 100 times that of fusion. It requires, however, a large energy investment and is expensive to manufacture (~ 100 billion dollars per gram (100B\$/g) assuming commercial electricity usage [Ref. 9]), and difficult to store and manipulate. While antiproton propulsion holds promise for the future, fission and fusion systems have the potential to provide quantum jumps in propulsive capability during the next fifty years of space exploration. It is these fuels upon which we will concentrate in this paper.

### Fission Fuels

Certain heavy elements such as uranium (U) and plutonium (Pu) are capable of undergoing a fission reaction when a critical amount of energy is supplied to the nucleus via a neutron absorption reaction (Ref.10). In a thermal reactor this energy is provided primarily by low energy neutrons (with energies in the range of ~0.01 eV to 0.3 eV; 1 eV=11,600 K), while epithermal and fast reactor configurations employ higher neutron energy spectrums. With the splitting of a typical fuel nucleus, such as U-235, a variety of reaction products are produced and considerable energy is released (~207 MeV). The reaction products include primary fission fragments and "prompt" neutrons and  $\gamma$ -rays (emitted at the instant of the fission event), and secondary radiation consisting of neutrinos,  $\gamma$ - and  $\beta$ -rays (released later as the fission fragments undergo radioactive decay). The bulk of the fission energy, ~168 MeV, appears as fission fragment kinetic energy and is collisionally dissipated in the fuel element material close to the site of the fission event. Neutron,  $\gamma$ - and  $\beta$ -ray energies (which total ~30 to 35 MeV) are also deposited within the reactor core providing a recoverable energy on the order of ~200 MeV per fission reaction.

Of the various fission products mentioned, the neutrons are the most important for they are essential for sustaining the fission chain reaction. The parameter  $\nu$  is used to indicate the average number of neutrons (both prompt and delayed) released per fission reaction. In a "critical" assembly at least one of these neutrons must induce an additional fission if the reactor is to continue to operate. The remaining ( $\nu-1$ ) neutrons are lost primarily through "parasitic" (non-fission) capture reactions, and neutron leakage. Because parasitic absorption can occur in fuel and structural materials alike the parameter  $\eta$  is often used to show how effectively neutrons are used in a reactor. Qualitatively  $\eta$  is equal to  $\nu$  times the relative probability that neutron absorption leads to fission. Quantitatively, it is given by

$$\eta = \nu / (1 + \alpha) \quad (1)$$

where  $\alpha (= \sigma_{\gamma} / \sigma_f)$  is the "capture-to-fission ratio" and  $\sigma_f$  and  $\sigma_{\gamma}$  are the fission and radiative capture cross sections, respectively.

Equation 1 is useful for evaluating the relative attractiveness of the various fission fuels, the most practical being the uranium isotopes, U-233 and U-235, and the plutonium isotope Pu-239. The thermal data for these isotopes and natural uranium, U-238, is shown in Table 2. The only naturally occurring isotope is U-235, which has a natural abundance of 0.71 atom percent. It can be extracted and enriched to

Table 2  
Thermal (0.025 eV) Data\* for U-233, U-235, U-238, and Pu-239

	$\sigma_a^+$	$\sigma_f$	$\alpha$	$\eta$	$\nu$
U-233	573	525	0.093	2.29	2.50
U-235	678	577	0.175	2.08	2.44
U-238	7.59	4.16	0.910	1.31	2.50
Pu-239	1015	741	0.370	2.12	2.90

\*From BNL-325, 2nd ed. (1958), Suppl. No. 2, Vol. III, Feb. 1965.

$$^+\sigma_a = \sigma_\gamma + \sigma_f$$

any desired level for reactor use by a variety of separation techniques. The isotopes U-233 and Pu-239 are produced by the absorption of neutrons by the abundant fertile isotopes thorium-232 (Th-232) and U-238. Pu-239 is used principally in the weapons program and its physical and chemical properties make it a difficult fuel to work with. Both U-233 and U-235 have been previously considered for use in nuclear rocket engines. With its large  $\nu$ -value and high probability of fission, a thermal reactor fueled with U-233 would require less fuel than one fueled with U-235. However, because there are no large scale facilities available for the production of U-233 this isotope is expected to be a more expensive fuel than U-235, which is the fuel of choice for first generation nuclear thermal rockets. Due to the limited reserves of U-235 and the abundance of thorium, U-233 could become an increasingly important nuclear fuel, finding use in both terrestrial "thermal breeder" reactors and extraterrestrial applications.

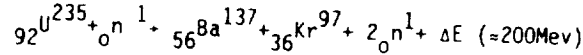
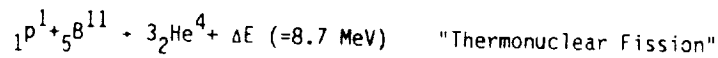
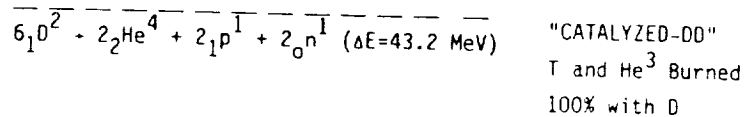
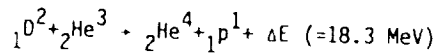
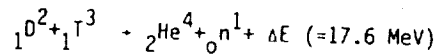
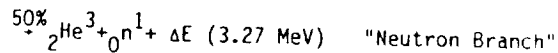
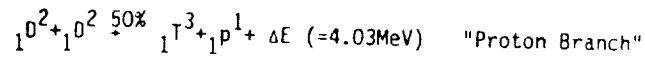
### Fusion Fuels

Table 3 shows the energy release and the reaction products for a sampling of fission and fusion nuclear fuels. Besides the fission process, nuclear energy can also be generated by fusing together various light elements; but this process requires that the temperature of the ionized mixture be sufficiently high (on the order of  $\sim 10^8$  to  $10^9$  K) for the positively charged fuel ions to overcome their Coulomb repulsion. The fuel cycles with the greatest reactivity at temperatures below 100 keV involve the hydrogen isotopes deuterium (D) and tritium (T) and the helium isotope He<sup>3</sup>. The energy liberated in the fusion process is partitioned among the reaction products [which include neutrons (n), hydrogen ions (p), and helium (He<sup>4</sup>)] in the form of kinetic energy.

The DT cycle has the largest reaction rate at low temperatures ( $\leq 15$  keV). Unfortunately, it releases 80% of its energy in the form of energetic (14.1 MeV) neutrons that can only be recovered in a complex

Table 3

## Released Energy and Products From Various Nuclear Reactions

"Typical" FissionFusion

tritium breeding blanket structure using thermal conversion equipment. Substantial quantities of shielding are also required for protection of crew and equipment (primarily the superconducting coils used to generate the plasma confining magnetic fields). The excessive weights involved in using DT appear to rule out its use for propulsion systems.

The DD fusion reaction is characterized by two branches that occur with equal probability: a "neutron" and a "proton" branch. By burning the tritium and He<sup>3</sup> resulting from these "energy poor" reactions in the DD plasma itself, a catalyzed DD (cat-DD) burn results that has a significantly improved energy output (~14.4 MeV/pair of DD fuel ions burned). In addition, greater than 60% of the energy output from a cat-DD reactor appears in the form of charged particles (protons and He<sup>4</sup>). The attractiveness of the cat-DD fuel cycle is that it is self sufficient, that is, it requires only naturally available deuterium as the main fuel feed. It is also relatively inexpensive (~1k\$/kg) [Ref. 11], and abundant (estimates of the deuterium content in the Earth's oceans and surface waters are placed at ~10<sup>13</sup> metric tons (mT); 1 mT = 1000 kg).

The DHe<sup>3</sup> reaction is particularly attractive for propulsion applications and has the largest power density of all the advanced fusion fuels over the temperature range of 45 - 100 keV. Neither of the fuel components are radioactive, and both of the reaction products - a 14.7 MeV proton and a 3.6 MeV He<sup>4</sup> nucleus, or alpha particle - are charged, making magnetic extraction and thrust generation possible.

The charged plasma can be either exhausted directly at high Isp ( $\sim 10^5$  to  $10^6$  s) or mixed with additional hydrogen reaction mass in a bundle divertor/magnetic nozzle for thrust augmentation at lower specific impulse ( $\geq 10^4$  s). This interchangeability of thrust and Isp is one of the potential operational advantages of fusion propulsion.

In addition to its relative cleanliness ( $< 5\%$  neutron power produced via DD side reactions), the DHe<sup>3</sup> cycle has an appreciable energy yield with a kilogram of equimolar DHe<sup>3</sup> producing  $\sim 25$  million times more energy than an equivalent amount of LO<sub>2</sub>/LH<sub>2</sub>. Until recently, the problem with the DHe<sup>3</sup> cycle has been the lack of abundant natural He<sup>3</sup> on Earth. This has changed with the identification of a potentially abundant source of He<sup>3</sup> ( $\sim 10^6$  mT) deposited on the lunar surface by solar wind bombardment [Ref. 12]. It is estimated that this reserve could provide adequate He<sup>3</sup> for both propulsion and power production for many decades or until such time as the vast reserves ( $\sim 10^{20}$  mT) of He<sup>3</sup> from Jupiter can be tapped [Ref. 12].

A final item of significance that could impact future DHe<sup>3</sup> usage deals with recent theoretical and experimental work [Ref. 13,14] on the use of "spin-polarized" fusion fuels. Indications are that spin polarization of the DHe<sup>3</sup> nuclei prior to reactor injection can enhance the fuel's reactivity by 50% while simultaneously suppressing the troublesome neutron-producing DD side reactions. If the perceived benefits of spin-polarized fuel are borne out in future experiments, a clean, fusion-powered, manned planetary transportation system could be available in the first half of the 21st century. Finally, on a longer time scale, the proton-based pB<sup>11</sup> (boron-11 isotope) fuel cycle could lead to a "superclean" fusion engine that exhausts only He<sup>4</sup> nuclei. The p-B<sup>11</sup> reaction might almost be termed a "thermonuclear fission reaction" in the sense that the B<sup>11</sup> nucleus is split into three alpha particles that are emitted with continuum energy spectrum.

## SOLID CORE FISSION THERMAL ROCKETS

### Solid Core Concepts

A variety of fission thermal rocket designs based on solid and gaseous core reactor concepts were studied during the Rover/NERVA program. From an evolutionary standpoint the solid core systems were considered to be the logical first step toward achieving a working nuclear rocket engine. These systems would be followed by the more advanced gaseous core engines capable of operating in the multi-kilosecond Isp regime. In the solid core reactor designs proposed in the late 1950's and early 60's, the fissioning uranium was contained in a variety of fuel element forms ranging from prismatic graphite assemblies to packed beds of particulate fuel spheres to the thin ribbed tungsten plates used in the Dumbo reactor concept [Ref. 15]. Thermal energy generated in the fuel elements by the fission process would be transmitted via heat conduction to a working fluid flowing through or over these fuel elements. The reactor coolant, heated to high temperatures, is then exhausted through a convergent-divergent nozzle at high velocities. The major components of a nuclear rocket engine are illustrated in Fig. 2.

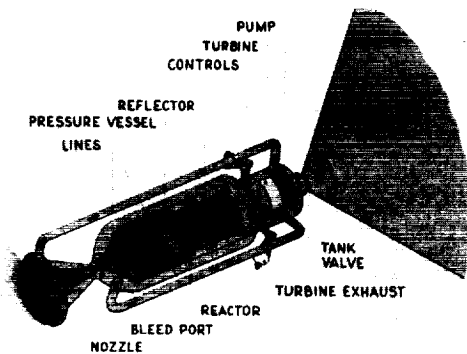


FIGURE 2. - SCHEMATIC OF A NUCLEAR ROCKET ENGINE EMPLOYING THE HOT-BLEED POWER CYCLE.

Because the square of the specific impulse is proportional to the rocket's propellant exit temperature divided by the molecular weight of the propellant, there is a strong incentive to use high melting point core materials to contain the fissioning uranium and to use hydrogen as the reactor coolant and propellant. The materials selected for use in the reactor fuel elements and structural components should, of course, have desirable high-temperature physical properties, possess a low thermal neutron absorption cross section, and be compatible with hydrogen over the fuel temperature range. Core designs using graphite, tungsten metal and carbides of hafnium and tantalum have been proposed and studied [Ref. 16].

The major emphasis in the Rover/NERVA program was on the graphite core concept. Graphite was selected because of its excellent high temperature strength, its availability, and its inherent neutron moderating capability. It also offered more promise for early engine development [Ref. 17]. A major disadvantage of graphite, however, is that it reacts with hot hydrogen to form methane and other gaseous hydrocarbons. The subsequent erosion and loss of graphite affects reactor neutronics and seriously limits the operational lifetime of the engine. This problem was surmounted by coating the graphite with carbides of niobium (NbC), and later zirconium (ZrC), to reduce hydrogen corrosion.

The basic fuel element structure used in the NERVA program is shown in Fig. 3. Particles of coated uranium carbide ( $UC_2$ ) were dispersed in a graphite matrix and an extrusion process was used to form the hexagonally-shaped fuel elements shown. Each element contained 19 coated coolant channels. An assembly of ~ 1100 of these elements would comprise the NERVA core. Near the program's end research in advanced materials and concepts led to the development of high expansion graphites with improved compatibility with carbide coatings, graphite-metal carbide composites (UC-ZrC-C) and pure carbides (UC-ZrC)-- fuel forms offering the potential for long duration (hours), high Isp operation (possibly in excess of 950 s for the pure carbides).

ORIGINAL PAGE IS  
OF POOR QUALITY

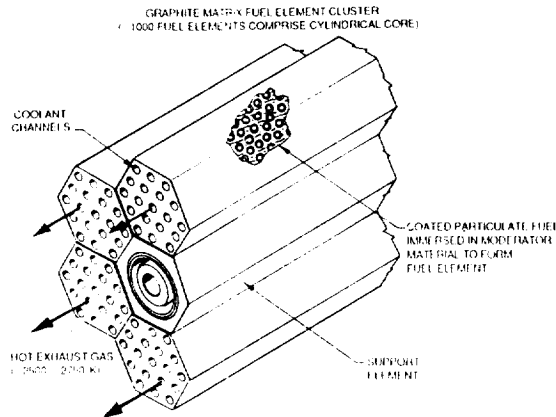


FIGURE 3. - ILLUSTRATION OF THE COATED-PARTICLE GRAPHITE MATRIX FUEL ELEMENT ASSEMBLY USED IN THE NERVA PROGRAM.

A limitation of the graphite element approach, is its low heat transfer capability. NERVA type reactors are relatively large and peak fuel power densities are limited to  $\sim 5000 \text{ MW/m}^3$ , due to the low surface to volume ratio of the core. A compact, high power density reactor concept developed by Brookhaven National Laboratory is currently under study by the U. S. Air Force for NOTV application. Referred to as the Particle Bed Reactor (PBR) concept [Ref. 18], its distinguishing feature is the direct cooling of small (500-700  $\mu\text{m}$  diameter) coated particulate fuel (CPF) spheres by the hydrogen propellant. A representative fuel element is shown in Fig. 4. The CPF is packed between two concentric porous cylinders, called "frits", which allow coolant penetration but firmly confine the particles in place. A number of these small annular fuel elements are arrayed in a

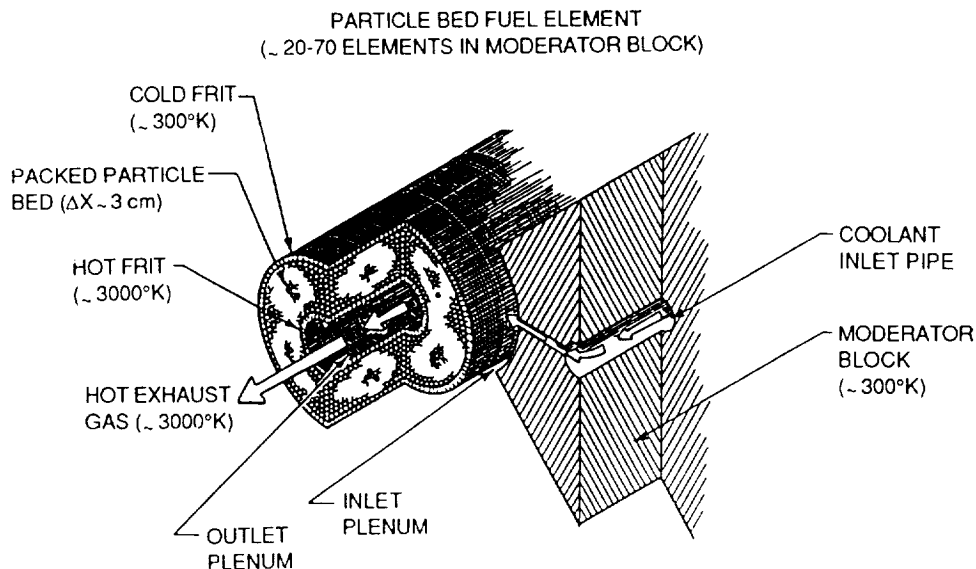


FIGURE 4. - TYPICAL FUEL ELEMENT AND MODERATOR BLOCK ASSEMBLY USED IN THE PBR CONCEPT. (COURTESY OF BROOKHAVEN NATIONAL LABORATORY).

cylindrical moderator block to form the PBR core. Because power generation in the PBR concept occurs only in the packed bed, the temperature of the moderator remains low (~300 K). Neutron and gamma heat deposited in the moderator during operation is removed by the hydrogen coolant before entering the inlet frit. Coolant flow is radially inward, through the packed bed and hot frit and axially out the inner annular channel at gas temperatures approaching 3000 K. Because of the large heat transfer area in the PBR element (~100 cm<sup>2</sup>/cm<sup>3</sup> of packed bed), bed power densities of ~10,000-50,000 MW/m<sup>3</sup> are possible. Such performance levels can lead to reactors having lower mass and physical size, and higher thrust-to-weight ratios.

### Operating Principles of the Solid Core Rocket

The basic components of a typical SCR utilizing the "hot-bleed" turbopump power cycle are shown in Fig. 2. The reactor consists of a cylindrical core containing fuel, moderator, and structure. The moderator consists of lightweight material such as graphite, beryllium, beryllium oxide, or various hydrides, which is placed in the reactor to insure a thermalized neutron flux. It can either be integral with the fuel element (as in the graphite NERVA reactor) or distinct from it (as in the PBR concept). The core is surrounded by an insulating shell and an additional region of moderating material called the reflector that reduces neutron leakage from the system by "reflecting" neutrons back into the core. Also contained within the reflector are a number of rotating drum elements used to regulate reactor power. These elements are made of the same material as the reflector except for a portion of the drum that is covered by a neutron absorbing material such as boron carbide. This two zone construction allows the control drums to act either as neutron reflectors or absorbers depending on which portion of the control drum faces the reactor core.

Because a fission thermal rocket produces a substantial neutron and gamma radiation field, a protective shield is normally placed between the reactor and sensitive engine components to prevent radiation heating and material damage. Lightweight low atomic number materials such as lithium hydride are used for neutron attenuation, while the more penetrating  $\gamma$ -rays are effectively handled by a denser material such as tungsten. To minimize its size and weight, the shield is positioned to intercept the largest possible solid angle as seen from the reactor. For the NERVA engine design the shield was placed above the reactor core. In this location heat produced by the neutron and gamma radiation could be extracted by the main propellant stream prior to entering the reactor core. Both the reactor and shield are contained in a pressure vessel on which is mounted a regeneratively cooled nozzle. Thrust is transferred through the reactor pressure vessel to the fuel tank structure and spacecraft.

During operation, liquid hydrogen from the propellant tank is pumped through a discharge line to a manifold at the nozzle exit. Flowing through cooling passages in the nozzle, the hydrogen is first directed upward through the reflector region and then downward through the internal shield and reactor core where it is heated to design

temperature. The hot gas exits into the nozzle plenum chamber and then the nozzle to produce thrust. A small portion of the hot hydrogen (~3%) is extracted through a bleed port to provide turbine drive gas. The temperature of the bleed gas is reduced to a level safe for turbine use by mixing it with a larger quantity of cold hydrogen. After passing through the turbine the gas is routed to two gimbed nozzles that use the discharge for vehicle roll control. The engine is started with a "bootstrap technique" [Ref. 19] using reactor heat capacity and tank pressurization gas for the initial turbine-fluid energy supply.

Because the exhaust temperature of the turbine gas is significantly lower than that of the main engine, an Isp performance penalty is incurred in using the hot bleed cycle. To improve the capability of the NERVA flight engine, later designs adopted the "full-flow topping cycle" [Ref. 20]. In this approach, the entire propellant flow, including the turbine drive fluid, is passed through the reactor core.

### Fuel Consumption and Fission Product Decay Issues

Due to the tremendous energy content of the fissionable fuel and the short duration of most high thrust propulsive maneuvers, SCRs consume only a minute portion of their available fuel inventory. Assuming primarily thermal-neutron induced fissions and U-235 fuel, this consumption rate is ~1.24 g/day per megawatt of power. Altseimer, et. al. [Ref. 20] have considered the NERVA flight engine ( $F = 334$  kN,  $P_{rx} = 1570$  MW,  $I_{sp} = 825$  s,  $\alpha = 85$  kW/kg) for use in a reusable Earth-lunar shuttle. The total  $P_{rx}$  burn duration at full power for the round trip mission was estimated at 43.1 minutes. Only 58 g of U-235 is consumed. Because the critical fuel loading at the 1500 MW level is on the order of several hundred kg, less than a 0.1% of the fuel is used in such a mission.

Following shutdown, significant heat continues to be generated in the core of a nuclear rocket due to  $\beta$ - and  $\gamma$ - decay of fission fragments. Reactor afterheat (which decreases with time) must be removed from the system in order to prevent structural damage to the fuel and the release of radiologically hazardous isotopes into space. Estimates of the decay afterheat can be obtained from the Borst-Wheeler relationship [Ref. 10]:

$$P_d(t,T) = 6.57 \times 10^{-2} [t^{-0.2} - (t+T)^{-0.2}] P_{rx} \quad (2)$$

Here  $P_d(t,T)$  is the decay power emitted in the form of  $\beta$ - and  $\gamma$ -rays by the  $P_{rx}$  fission product inventory of a reactor that has been operated for T seconds at a power  $P_{rx}$ , t seconds after it has been shut down. Following a 25 min. translunar insertion burn by the NERVA-based lunar shuttle of Ref. 20, Eq. (2) indicates that the afterheat power level will be ~ 1.35 MW one hour after engine operation. This value will drop to 36.5 kW after 24 hours and ~ 10 kW after 72 hours.

In SCR systems the nuclear decay heat should be removed at the highest possible Isp to insure coolant economy. This is accomplished by reducing chamber pressure and passing propellant through the engine in discrete pulses [Refs. 19, 20]. A small level of continuous flow is

used early on in the cooldown phase to prevent overheating of certain core components. The frequency of the coolant pulses will decrease with time, until the decay heat reaches the 10 kW level at which point the engine is capable of radiatively dissipating the remaining energy. Thrust generated during the cooldown period is not wasted but contributes to the total velocity requirements of the mission. Because it is a predictable quantity, its use can be integrated into the overall mission profile to provide trajectory correction or trimming velocity.

Additional propellant savings were found to be possible by employing a "dual mode" engine configuration in which the SCR provides a source of energy for both primary propulsion and long-duration electrical power generation. A dual mode nuclear rocket engine design has been analyzed by Beveridge [Ref. 21] for use on the NERVA engine. The design employs a separate, closed-loop organic Rankine cycle with thiophene as the working fluid. Waste heat is dissipated using a radiator system incorporated into the surface of the propulsion module coolant tank. By operating the reactor at low power levels (~200 kW) during the non-thrusting portion of the mission, ~25 kW of electrical power can be generated continuously for recharging batteries, as well as navigation and communications operations. More importantly, by using the auxiliary plant to cool the reactor after each propulsive maneuver, it is possible to reduce both the amount and duration of cooldown hydrogen flow by ~50% and 90%, respectively. For all NERVA missions studied [Ref. 21], it was found that the savings in cooldown propellant more than compensated for the additional weight of the auxiliary power system (~ 2.7 mT).

#### Accomplishments of the Rover/NERVA Program

The basic research and technology development required to build a flight-rated solid core rocket engine was essentially in hand at the completion of the Rover/NERVA program in 1973. During the years 1959 through 1972 a total of nineteen reactors were built and tested at various power levels (Fig. 5). Phoebus-2A was the most powerful nuclear rocket reactor ever constructed [Ref. 2]. Designed for 5000 MW, the reactor had a nominal thrust of 1110 kN (250,000 lbf) and an Isp of 840 s. Phoebus-2A was intended to be the prototype for NERVA-2 [Ref. 22], a 200,000 - 250,000 lbf optimum-thrust engine to be used for manned missions to Mars. Because of inadequate cooling to a portion of its aluminum pressure vessel, actual reactor operation was limited to ~80% of rated power. Even at this reduced level Phoebus demonstrated record performance in the areas of power (~4100 MW), thrust (930 kN), hydrogen flow rate (~120 kg/s), and minimum reactor specific mass (~2.3 kg/MW).

Equally impressive results were achieved in the smaller research reactors, Pewee and the Nuclear Furnace (NF), designed primarily as test beds for evaluation of various fuel<sub>3</sub> element designs. Pewee set records in peak power density (5200 MW/m<sup>3</sup>), exit gas temperature (2550 K) and specific impulse (845 s) while the much smaller NF reactor operated for a record time of 109 min. with an exit gas temperature of <sub>3</sub>~2450 K and peak fuel power densities in the range of 4500-5000 MW/m<sup>3</sup>. More importantly, this performance level was achieved using the advanced composite and pure carbide fuel element

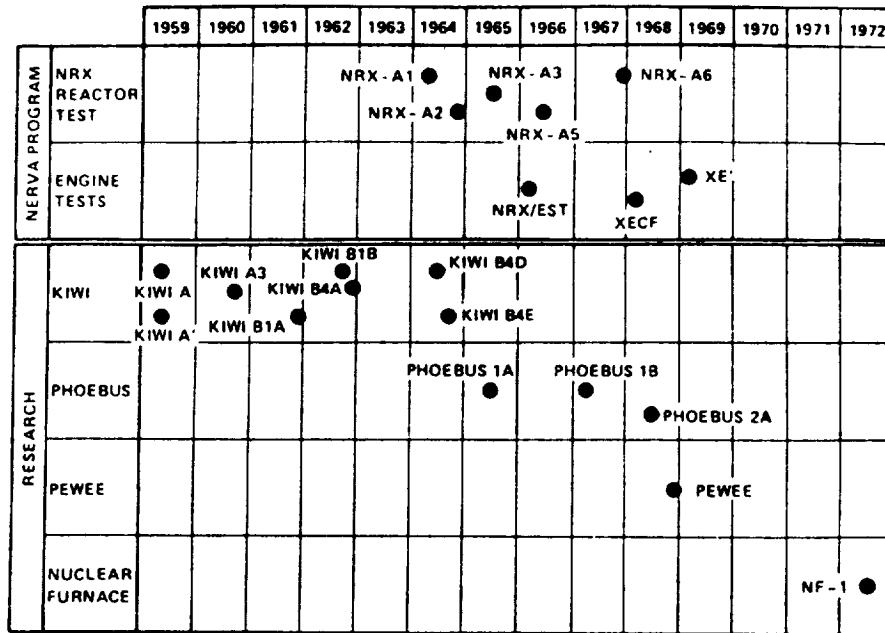


FIGURE 5. - SUMMARY OF MAJOR NUCLEAR ROCKET TESTS CONDUCTED DURING THE ROVER AND NERVA PROGRAMS (REF. 21).

designs that were developed for the purpose of improving engine lifetime. On the basis of data obtained from the NF and additional electrical furnace tests [Ref. 23], operational lifetimes of ~10 hours were shown to be feasible (Fig. 6).

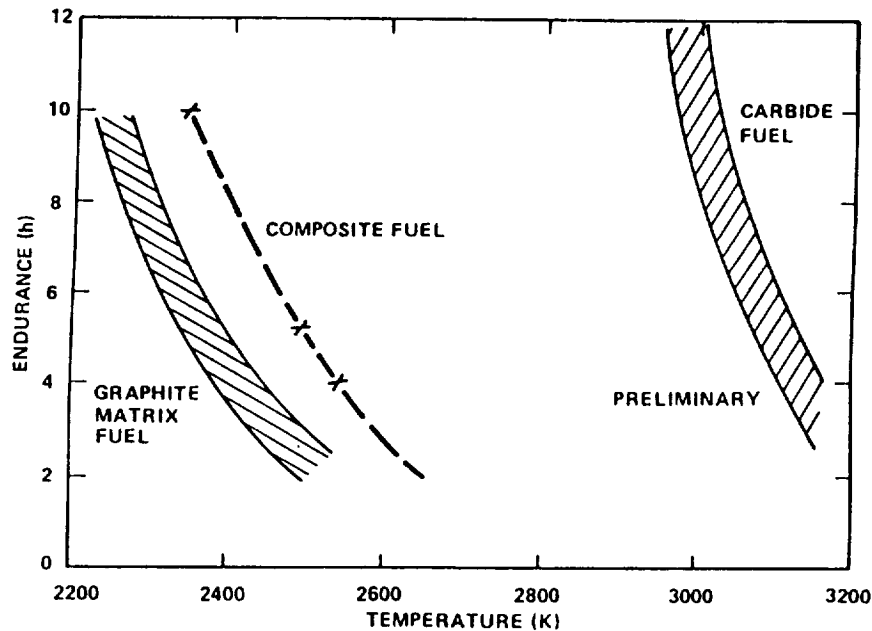


FIGURE 6. - PROJECTED LIFETIMES OF VARIOUS FUELS VERSUS COOLANT EXIT TEMPERATURE (REF. 21).

In addition to the Kiwi, Pewee, Phoebus and NF reactors built during the Rover research program, five 1100 MW reactors were operated in the NERVA program under the Nuclear Reactor Experiment (NRX) test series. Among these reactors the NRX-A6 ran continuously for 62 min. at 1125 MW and an equivalent vacuum Isp of 730 s. Nuclear and nonnuclear flight components were fully integrated into a prototype nuclear engine configuration in the XE-P system shown in Fig. 7. The XE consisted of two parts; a lower module containing the reactor, pressure vessel, nozzle and control drum actuators, and an upper module that contained the turbopump assembly, feed lines and valving. Protection of radiation sensitive components in the upper module was provided by an external shield that was also used to transmit loads from the lower to upper thrust structures. In the NERVA flight engine the external shield was not an integral part of the thrust structure and was designed for complete removal and reinstallation in space.

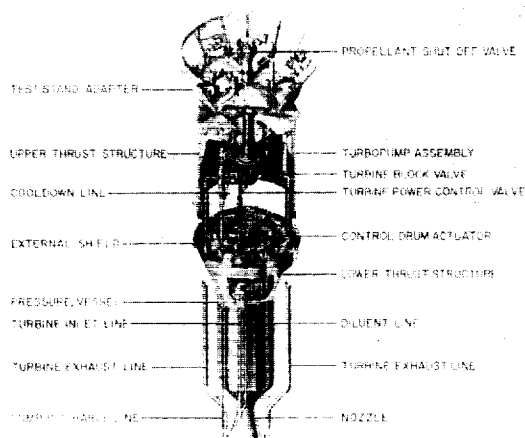


FIGURE 7. - CUTAWAY VIEW OF THE XE-P ENGINE. (COURTESY OF AEROJET TECHSYSTEMS COMPANY).

The XE engine (Fig. 8) underwent an extensive series of tests under partial vacuum conditions in the engine test facility (ETS-1) located at the Nuclear Rocket Development Station in Nevada. The engine operated successfully at rated power (1140 MW) producing a nominal thrust of 245 kN (55,000 lbf) at a chamber temperature and pressure of 2270 K and 3.86 MPa (560 psia), respectively. The total engine flow rate was 36 kg/s and the overall Isp was 715 s under partial vacuum (~1 psia in ETS-1). The XE was successfully started a record 24 times [Ref. 24] and accumulated a total of 115 min of powered operation. Engine restart was demonstrated even with maximum xenon poisoning present in the core [Ref. 25]--a capability attributed to the XE's neutron energy spectrum that was faster than thermal yet still provided the inherent safety and thermal stability features of thermal reactors. A number of candidate control concepts under consideration for the NERVA flight engine were also evaluated and completely automatic startup capability was demonstrated. The XE test series proved convincingly that a nuclear rocket engine could be started, operated, shutdown, and restarted in a well-controlled manner over the wide range of reactor conditions that could be encountered in flight.

ORIGINAL PAGE IS  
OF POOR QUALITY

ORIGINAL PAGE IS  
OF POOR QUALITY



FIGURE 8. - VIEW OF THE XE BEING INSTALLED IN THE ETS-1 FACILITY. (COURTESY OF AEROJET TECHSYSTEMS COMPANY).

#### GAS CORE FISSION THERMAL ROCKETS

The temperature limitations imposed on the solid core thermal rocket designs by the need to avoid material melting can be overcome, in principle, by allowing the nuclear fuel to exist in a high temperature (10,000 - 100,000 K), partially ionized plasma state. In this so-called "gaseous- or plasma-core" concept, an incandescent cylinder or sphere of fissioning uranium plasma functions as the fuel element. Nuclear heat released within the plasma and dissipated as thermal radiation from its surface is absorbed by a surrounding envelope of seeded hydrogen propellant that is then expanded through a nozzle to provide thrust. Propellant seeding (with small amounts of graphite or tungsten powder) is necessary to insure that the thermal radiation is absorbed predominantly by the hydrogen and not by the cavity walls that surround the plasma. With the gas core rocket (GCR) concept Isp values ranging from 1500 to 7000 s appear to be feasible [Ref. 26]. Of the various ideas proposed for a gas core engine, two concepts have emerged that have considerable promise: an open cycle configuration, where the uranium plasma is in direct contact with the hydrogen propellant, and a closed-cycle approach, known as the "nuclear light bulb engine" concept, which isolates the plasma from the propellant by means of a transparent, cooled solid barrier.

#### Porous Wall Gas Core Engine

The "open cycle," or "porous wall," gas core rocket is illustrated in Fig. 9. It is basically spherical in shape and consists of three solid regions: an outer pressure vessel, a neutron reflector/moderator region and an inner porous liner. Beryllium oxide ( $\text{BeO}$ ) is

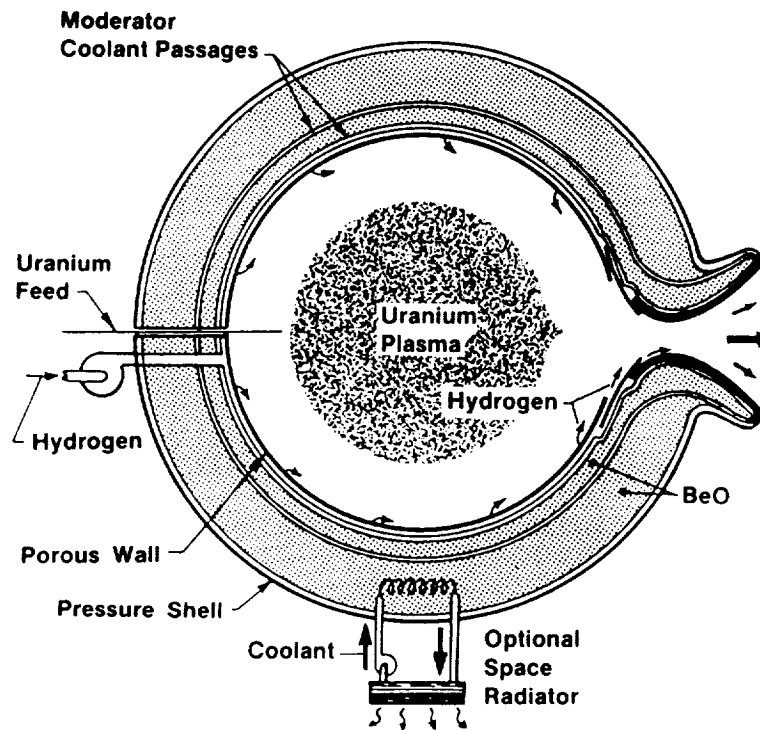


FIGURE 9. - HIGH SPECIFIC IMPULSE, POROUS WALL GAS CORE ENGINE. (COURTESY OF NASA, LEWIS RESEARCH CENTER).

selected for the moderator material because of its high operating temperature and its compatibility with hydrogen. The open cycle GCR requires a relatively high pressure plasma (500 - 2000 atm;  $1 \text{ atm} = 1.013 \times 10^5 \text{ N/m}^2$ ) to achieve a critical mass. At these pressures the gaseous fuel is also dense enough for the fission fragment stopping distance to be comparable to or smaller than the dimensions of the fuel volume contained within the reactor cavity. Hydrogen propellant, after being ducted through the outer reactor shell, is injected through the porous wall with a flow distribution that creates a relatively stagnant non-recirculating central fuel region in the cavity. A small amount of fissionable fuel (1/4 to 1 % by mass of the hydrogen flow rate) is exhausted, however, along with the heated propellant.

Because the uranium plasma and hot hydrogen are essentially transparent to the high energy gamma rays and neutrons produced during the fission process, the energy content of this radiation (~7-10% of the total reactor power) is deposited principally in the solid regions of the reactor shell. It is the ability to remove this energy, either with an external space radiator or regeneratively using the hydrogen propellant, that determines the maximum power output and achievable Isp for the GCR engines. To illustrate this point, an open cycle engine with a thrust rating of 220 kN (50,000 lbf) is considered. We assume that 7% of  $P_{\text{rx}}$  reaches the solid, temperature-limited portion of the engine and that the remainder is converted to jet power at an

isentropic nozzle expansion efficiency of  $\eta_j$ . Based on the relationships between Isp, reactor power and propellant flow rate ( $\dot{m}_p$ ) given below

$$0.93P_{rx} \text{ (MW)} = \begin{cases} 4.9 \times 10^{-6} F(N) I_{sp}(s) / \eta_j & (3a) \\ 4.8 \times 10^{-5} \dot{m}_p \text{ (kg/s)} I_{sp}^2(s) / \eta_j & (3b) \end{cases}$$

a 5000 s engine generating 7500 MW of reactor power will require a flow rate of 4.5 kg/s at rated thrust. If the hydrogen is brought into the cavity at a maximum overall operating temperature of 1400 K, no more than 1.2% of the total reactor power (~17% of the neutron and gamma power deposited in the reactor structure) can be removed regeneratively ( $\dot{m}_c \Delta T \approx 90$  MW). Total removal requires either (1) operating the solid portions of the engine at unrealistically high temperatures (>11,000 K at  $\dot{m}_p = 4.5$  kg/s) or (2) increasing the propellant flow rate substantially to 36.8 kg/s (at 1400 K), which reduces the engine's Isp to 1750 s. "Closed cooling cycle" space radiator systems have been proposed [Ref. 27] as a means of maintaining the GCR's operational flexibility. With such a system, adequate engine cooling is possible even during high Isp operation when the hydrogen flow is reduced. Calculations performed by NASA/Lewis Research Center [Ref. 28] indicate that specific impulses ranging from 3000 to 7000 s could be attained in radiator-cooled, porous wall gas core engines.

The performance and engine characteristics for a 5000 s class of open cycle GCRs are summarized in Table 4 for a range of thrust levels. The diameter of the reactor cavity and the thickness of the external

Table 4  
Characteristics of 5000 s Porous Wall Gas Core Rocket Engines

F(kN)	$P_{rx}$ (MW)	$P_{rad}$ (MW) <sup>a</sup>	$M_w$ (mT)	$M_{pv}$ (mT) <sup>b</sup>	$M_{rad}$ (mT) <sup>c</sup>	$M_{mod}$ (mT) <sup>d</sup>	$\alpha_p$ (kW/kg)	$F/M_w$
22	750	43.5	52.3	10	6.3	36	10.3	$4.3 \times 10^{-2}$
44	1500	87	61.6	13	12.6	36	17.5	$7.3 \times 10^{-2}$
110	3750	218	86	18	32	36	31.3	0.13
220	7500	435	123	24	63	36	43.8	0.18
440	15000	870	193	31	126	36	55.9	0.23

<sup>a</sup> For a hydrogen cavity inlet temperature of 1400 K and a heat deposition rate that is 7% of the reactor power, the ratio of radiated to total reactor power is a constant equal to 5.8%.

<sup>b</sup> The weight of the spherical pressure vessel is based on a strength-to-density value of  $1.7 \times 10^5$  N·m/kg [Ref. 29] which is characteristic of high strength steels.

<sup>c</sup> Used in these estimates is a radiator specific mass of 145 kg/MW [Ref. 28] which is based on a heat rejection temperature of 1225 K and a radiator weight per unit surface area of  $19 \text{ kg/m}^2$ .

<sup>d</sup> Density of BeO is  $2.96 \text{ mT/m}^3$ .

reflector/moderator region are fixed at 2.44 m and 0.46 m, respectively, which represents a near-optimum engine configuration. The engine weight ( $M_w$ ) is composed primarily of the pressure vessel ( $M_{pv}$ ); radiator ( $M_{rad}$ ); and moderator ( $M_{mod}$ ).

By fixing the engine geometry in Table 4 the mass of the BeO moderator remains constant at 36 mT. However, the pressure vessel and radiator weights are both affected by the thrust level. While the radiator weight increases in proportion to the extra power that must be dissipated at higher thrust, the reason for the increase in pressure vessel weight is slightly more subtle. For a constant Isp engine an increase in thrust is achieved by increasing both the reactor power and hydrogen flow rate. In order to radiatively transfer this higher power to the propellant, the uranium fuel temperature increases, necessitating an increase in reactor pressure to maintain a constant critical mass in the engine. Accommodating this increased pressure leads to a heavier pressure vessel. (In going from 22 kN to 440 kN, the engine pressure rises from 570 atm to 1780 atm).

As Table 4 illustrates, the moderator is the major weight component at lower thrust levels (<110 kN) while the radiator becomes increasingly more important at higher thrust. At thrust levels of 220 kN and above, the radiator accounts for more than 50% of the total engine weight. There is therefore a strong incentive to develop high temperature (~1500 K) liquid metal heat pipe radiators that could provide significant weight reductions in the higher thrust engines.

Table 4 also shows an impressive range of specific powers and engine thrust-to-weight ratios for the thrust levels examined. The  $F/M_w$  ratio for the 22 kN engine is over two orders of magnitude higher than the 5000 s nuclear-powered MPD electric propulsion system proposed in the Pegasus study [Ref. 30]. For manned Mars missions the higher acceleration levels possible with the GCR can lead to significant (factor of 5) reductions in trip time compared to the Pegasus system.

#### Nuclear Light Bulb Engine

In the closed-cycle nuclear light bulb engine concept [Ref. 31], thermal radiation is transferred from the gaseous fuel to the seeded hydrogen through an internally cooled transparent wall that physically isolates the uranium fuel and fission products from the propellant exhaust. The wall material is constructed of silicon or beryllium oxide. Sketches of the engine illustrating its operational principles are given in Fig. 10. The uranium fuel is prevented from condensing on the cooled wall by a vortex flow field created by the tangential injection of a neon "buffer" gas near the inside surface of the transparent wall. Neon discharged from the system exits through ports located on the centerline of the forward cavity wall and passes to a fuel recycle system. Here fission products are removed and the nuclear fuel entrained in the neon is condensed to liquid form, centrifugally separated from the neon, and pumped back into the fuel region of the vortex. The neon is also pumped back into the cavity to drive the vortex. This closed-cycle fuel system provides the light bulb engine with its most attractive feature - complete containment of unburned fuel and fission products.

ORIGINAL PAGE IS  
OF POOR QUALITY

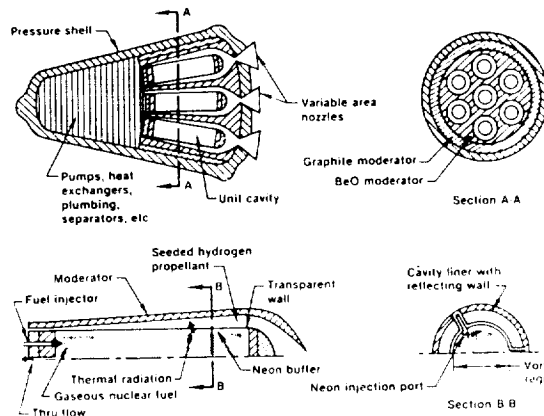


FIGURE 10. - SKETCHES ILLUSTRATING THE OPERATION PRINCIPLES OF THE NUCLEAR LIGHT BULB ENGINE (REF. 31).

A reference design [Ref. 32] for the nuclear light bulb engine was established that consisted of seven cylindrical cavities (Fig. 10). The engine produced a total power of 4600 MW and operated with a hydrogen flow rate and Isp of 220 kg/s and 1870 s, respectively. The resulting engine thrust was 410 kN (~92,000 lbf). Engine weight was estimated to be ~ 31.3 mT and was made up of the following component weights: moderator (graphite and BeO), 12.3 mT; pressure vessel, 13.6 mT; turbopumps, 1.4 mT; and miscellaneous (including the fuel recycle system), 4.5 mT. Heat extracted from the pressure vessel, cavity liner tubes and transparent walls was used to drive the fuel and propellant pumps while energy deposited in the moderator was removed regeneratively using the primary hydrogen propellant. With the addition of a space radiator, system studies [Ref. 32] showed that Isp's as high as 3200 s were achievable.

#### Status of GCR Experimental Research

The gas core research program conducted extensive experimental tests between 1961 and 1973 aimed at simulating the functional details of a gas core reactor. The three principle areas of investigation involved gaseous fuel criticality, fluid mechanical confinement of a nuclear fuel, and propellant heating via radiative heat transfer. Although most of the experimental work in the gas core program ended over a decade ago, the important features of both concepts were successfully demonstrated in individual as well as combined experiments. Extensive criticality experiments were conducted at the Idaho National Reactor Test Station [Ref. 33, 34] to measure the critical mass of various cavity reactor configurations. The criticality of gaseous uranium hexafluoride ( $UF_6$ ) was demonstrated in a cold-static configuration at zero power in both cylindrical and spherical geometries. These static tests were later followed by criticality experiments in a cold-flowing configuration [Ref. 35]. Neutronics codes, benchmarked against this experimental data, were subsequently used to predict the critical mass requirements for both gas core engine concepts.

Fluid mechanics research was of central importance to both the open cycle and nuclear light bulb engine programs because of their reliance on fluid mechanical techniques for minimizing fuel loss and maintaining wall transparency against uranium condensation. In the

open cycle program, cold-flow experiments demonstrated that relatively large, stable fuel-rich volume could be established and maintained within a spherical, porous-wall test cavity using a high velocity propellant flow. Propellant-to-fuel mass flow rate ratios in the range of 100 to 400 [Ref. 36] were also achieved in these experiments.

While these cold-flow tests provided data relevant to reactor flow conditions during engine startup, additional information was required to determine if hot, heat-generating plasmas exhibited the same general flow characteristics as the cold flows. A number of hot plasma flow experiments were conducted using electrical induction heating to generate a small rf discharge in the central region of the flow to simulate the gaseous nuclear fuel. Both argon and uranium plasmas were studied at electrical power levels of 1 MW. With ~600 kW generated in the plasma, the volumetric heating rate was ~900 MW/m<sup>3</sup>, a value comparable to the fission<sub>3</sub> power densities anticipated in operational GCRs (400-4000 MW/m<sup>3</sup>). In the rf heated uranium plasma experiments, a solid uranium wire was used to feed the plasma -- the same technique being considered for an operational engine (Fig. 9). Results from the various hot flow experiments were very encouraging, indicating that fuel confinement was as good as, if not better than, the cold flow results.

Hot flow experiments were also carried out in the nuclear light bulb program [Ref. 31], with induction heated plasmas providing an intense, non-nuclear radiation power source for testing transparent wall models and for simulating seeded propellant heating by thermal radiation. The transparent wall models that were developed consisted of cylindrical arrays of thin walled, axial coolant tubes [Ref.31] made of fused silica. Tangential injection of an argon buffer gas between the silica tubes and the plasma discharge was provided by injector assemblies built into the wall model. At discharge power levels of ~50 kW, the fused silica tubing sustained heat deposition rates on its inside surface as high as 340 W/cm<sup>2</sup> (a factor of 2 higher than that expected in the reference engine) with no apparent damage.

Significant progress was also made in the area of propellant heating. Using thermal radiation from a low power arc heated plasma, a seeded simulated propellant (argon with micron-sized carbon particles) was heated to exit temperatures ranging from 1700 to 2700 K [Ref. 37]. In these experiments the seed material in the propellant was responsible for attenuating nearly 90% of the radiant energy emitted from the argon source plasma.

While most experimental work on GCRs ended with the Rover/NERVA program, there is currently renewed interest in the feasibility of a gas core reactor and its use for space nuclear power. Experimental work being conducted at the California State University [Ref. 38], under sponsorship of the Strategic Defense Initiative Office, is aimed at recreating and extending the fluid mechanical confinement results obtained in the open cycle research program. Continued support for this work could lead to the development of a reactor with tremendous potential for both space propulsion and power.

## FUSION PROPULSION CONCEPTS

Rocket propulsion driven by thermonuclear fusion reactions is an attractive concept: a large amount of energy can be released from a relatively small amount of fuel, and the charged reaction products can be manipulated electromagnetically for thrust generation. Propulsion systems deriving their energy from high energy density fusion fuels have the potential to simultaneously demonstrate large exhaust velocities and high jet powers that could make Solar-System-wide travel feasible. These advanced propulsion reactors will be quite complex, however, and must be designed to be portable, compact, and self-contained. These criteria will necessitate the development of lightweight, high strength materials for use in the primary reactor and its auxiliary systems.

### Magnetic Confinement Fusion

Fusion reactors based on the magnetic confinement concept use superconducting coils to generate the strong magnetic fields needed to confine and isolate the ultrahot power-producing plasma from the reaction chamber walls. The fusion plasma, consisting of positively charged fuel ions and negatively charged free electrons, has a kinetic pressure that can be expressed as a percentage of the confining magnetic field pressure through the use of the local "plasma beta value",  $\beta$ , defined (in MKS units with T in keV) by

$$\beta = 2\mu_0(n_e kT_e + n_i kT_i)/B^2 \quad (4)$$

The parameters  $n_{e(i)}$ ,  $T_{e(i)}$ , and B are the electron (ion) particle density, temperature, and magnetic field strength, respectively. The constant  $k = 1.602 \times 10^{-16}$  J/keV and  $\mu_0$  is the permeability of free space. The power density in a fusion reactor is given by

$$P_f/V_p = \alpha_{jk} n_j n_k \langle \sigma_{jk} v \rangle k Q_{jk} ; \alpha_{jk} = \begin{cases} 1 & ; j \neq k \\ 1/2 & ; j = k \end{cases} \quad (5)$$

where  $P_f$  and  $V_p$  are the fusion power and plasma volume,  $n_j, n_k$  are the respective densities of the two reacting ion species,  $\langle \sigma v \rangle$  is the Maxwellian-averaged fusion reactivity (Fig. 11) and  $Q_{jk}$  is the energy release per  $jk$  reaction (appears as  $\Delta E$  in Table 2). Assuming  $n_e = n_i$ ,  $T_e = T_i$ ,  $\alpha_{jk} = 1$ , and  $n_j = n_k = n_i/2$  (a 50/50 fuel mix), Eq. (5) can be rewritten as

$$P_f/V_p = k' \beta^2 B^4 [\langle \sigma_{jk} v \rangle / T_i^2] Q_{jk} \quad (6)$$

where  $k' = 6.18 \times 10^{25}$ . Equation (6) shows that for a maximum magnetic field strength capability and optimal operating temperature (where  $\langle \sigma v \rangle / T_i^2$  is a maximum), the fusion power density scales like  $\beta^2$ . There is therefore a strong incentive to develop MCF concepts that operate at high  $\beta$ .

While a number of such concepts do exist, their developmental status at this time is substantially behind that of the mainline concepts such as the tokamak. One possible candidate MCF system that could be

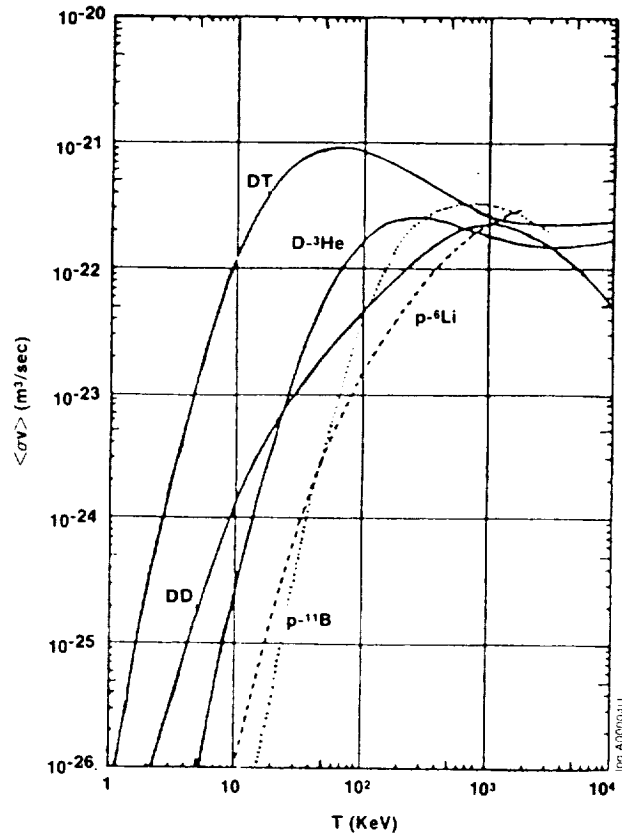


FIGURE 11. - COMPARISON OF DT AND ADVANCED FUEL REACTIVITIES.

developed for propulsion applications is based on an advanced tokamak concept known as the Spherical Torus (ST) [Ref. 39]. Before discussing its propulsion potential, however, a brief discussion of the basic tokamak concept and its performance are in order.

#### The Tokamak Concept and its Achievements to Date

The tokamak is the world's leading magnetic confinement fusion concept involving a worldwide investment by the U.S., Europe, Japan, and the USSR estimated at between 1 and 2B\$ annually. The basic device (illustrated in Fig. 12) is toroidal, consisting of a hollow vacuum vessel for the production and confinement of large volumes of high-temperature plasma. The donut-shaped plasma is immersed in a helically twisted magnetic field formed through the combination of a strong toroidal field (produced by a set of toroidal field coils which wrap around the torus) and a weaker poloidal field component (produced by the current flowing through the plasma itself). This plasma current can be driven either inductively by transformer action or noninductively by injected radiofrequency (rf) waves [Ref. 40]. A cross section of the tokamak's magnetic field structure yields a set of nested poloidal magnetic field surfaces. It is on these surfaces that the circulating hot plasma particles are confined and across which they conduct heat and collisionally diffuse.

ORIGINAL PAGE IS  
OF POOR QUALITY

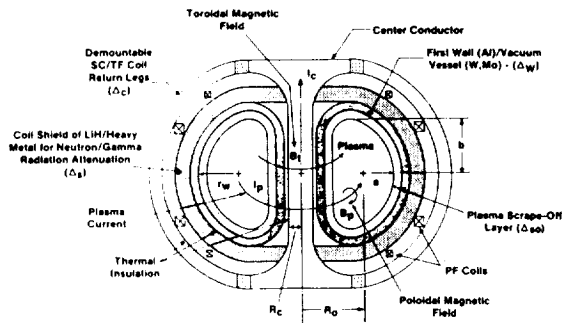


FIGURE 12. - SCHEMATIC OF AN ADVANCED (SPHERICAL TORUS) TOKAMAK REACTOR SYSTEM.

Ohmic heating (associated with the plasma's collisional resistance to current flow) and auxiliary heating (in the form of injected beams of energetic neutral atoms or rf wave energy) are used to increase the plasma temperature so that the fuel nuclei can overcome their mutual Coulomb repulsive force and fuse. At sufficiently high temperatures, the plasma will ignite, i.e., its reactivity increases to the point where the power of the charged fusion reaction products ( $P_{cp}$ ) alone can maintain the fusing plasma temperature against losses associated with radiation [both bremsstrahlung ( $P_{brems}$ ) and synchrotron ( $P_{synch}$ )] and transport mechanisms. Exhausting this transport power ( $P_{tr}$ ) for thrust generation and thermally converting the radiation loss ( $P_{tr}$ ) (which can also include neutron radiation) for needed recirculation power are the key elements of a self-sustaining tokamak fusion rocket (see Fig. 13).

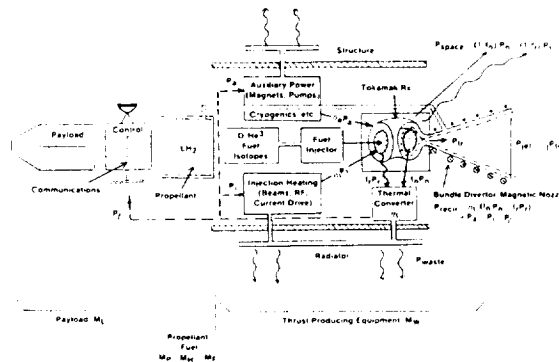


FIGURE 13. - COMPONENT AND POWER FLOW DIAGRAM FOR AN ADVANCED TOKAMAK FUSION ROCKET.

Steady progress has been maintained worldwide in tokamak plasma physics understanding and technology development. Breakeven-size tokamaks are currently operating in the U.S. (Princeton's Tokamak Fusion Test Reactor), England (the Joint European Torus sited at Culham Laboratories), Japan (the Japanese Tokamak-60), and the USSR (the superconducting T-15 tokamak), and expectations are high that energy breakeven, and possibly ignition, will be achieved in the TFTR and JET devices in the next 2 to 3 years.

The results obtained to date in TFTR and JET have been impressive. In TFTR, central ion temperatures of ~20 keV (13 times greater than that in the Sun's interior) have been obtained using 15 MW of neutral beam heating power [Ref. 41]. The corresponding "Lawson parameter"

[defined as the product of plasma density ( $n$ ) and energy confinement time ( $\tau_E$ )] was  $10^{13}$  s/cm<sup>3</sup> -- a value corresponding to unthermalized breakeven (see Fig. 14) had tritium been used as one of the fuel components. The much larger JET device, with a toroidal plasma volume of  $\sim 150$  m<sup>3</sup> compared to TFTR's 35 m<sup>3</sup>, has also made significant progress achieving plasma densities, temperatures, and energy confinement times of  $\sim 3-4 \times 10^{15}$ /cm<sup>3</sup>, 3-4 keV, and 0.8 s, respectively. When one compares these parameters with those required for an actual tokamak reactor [T $\sim$ 20 keV,  $n \sim 1-2 \times 10^{14}$ /cm<sup>3</sup>, and  $\tau_E \sim 1-2$  s assuming DT fuel], the outlook appears promising that a power producing system can be available within the first few decades of the 21st century. With this in mind, it is interesting to speculate on the use of a high-performance, steady-state tokamak reactor as a driver for a fusion rocket engine.

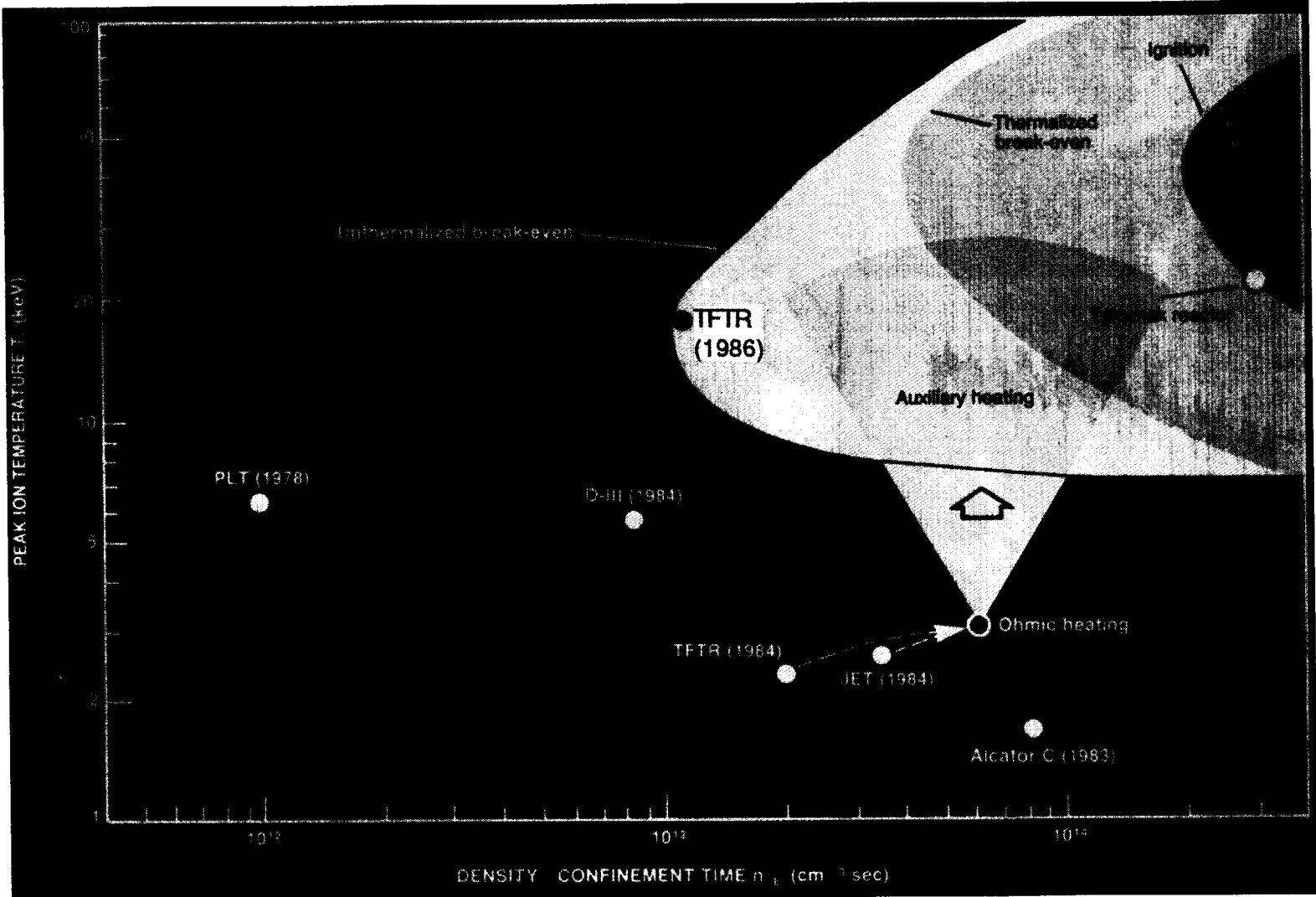
### Spherical Torus Fusion Rocket

In the ST concept, only what is absolutely indispensable inboard of the plasma is retained. This includes a first wall/vacuum chamber arrangement and a center conductor that carries current to produce the tokamak's toroidal magnetic field. Other components, such as an inner solenoid and inboard neutron shield are also eliminated. The resulting device has an exceptionally small aspect ratio\* ( $A \sim 1.5$  to 2 compared to  $\sim 3$  to 5 for a conventional tokamak) and looks much like a sphere with a modest hole through the center, hence the name spherical torus. While the small aspect ratio provides the ST with its high  $\beta$  potential ( $\beta \sim 20 - 40\%$ ), the lack of space in the torus inner bore rules out the use of a solenoid for inductive current startup and maintenance. Fortunately, tokamak experiments have demonstrated the feasibility of driving plasma currents noninductively [Refs. 40, 42] using injected rf wave energy, an important step that could lead to steady state tokamak operation.

Due to the absence of an inboard neutron shield in the ST concept, terrestrial reactor designs using DT fuel are prohibited from using a superconducting center conductor, and, instead, must employ a heavy, power-consuming resistive magnet. The potential for "neutronless" fusion power generation made possible through the use of spin-polarized DHe<sup>3</sup> has led the author to examine a high field ( $B_t \sim 10$  Tesla), superconducting version of the ST for rocket application [Ref. 43]. The configuration is illustrated in Fig. 12, and assumes the use of demountable superconducting (SC) Toroidal Field (TF) coil legs to improve access to the internal torus and poloidal field coils. The central conductor uses a high field / high current density ( $< 10^8$  A/m<sup>2</sup>) superconductor employing an "advanced" vanadium-gallium alloy (Va<sub>2</sub>Ga) and an aluminum stabilizer for weight reduction. A lightweight ( $\sim 2.7$  mT/m<sup>3</sup>), high strength (yield stress of 185 ksi) boron filament plastic is used for structural support against the various magnetic forces.

---

\*  $A = R_0 / a$  with  $R_0$  = torus major radius and  $a$  = plasma horizontal minor radius.



ORIGINAL PAGE IS  
OF POOR QUALITY

FIGURE 14. - FUSION PROGRESS CHART, SHOWING TOKAMAK EXPERIMENTS GETTING CLOSER TO THE FUSION REACTOR REGIME. (COURTESY OF PRINCETON PLASMA PHYSICS LABORATORY).

For the Spherical Torus-based fusion rocket (STR) to operate continuously and at high power output, it is necessary to remove the non-fusionable thermalized charged particle "ash" (protons and He<sup>4</sup> ions) from the plasma. The magnetic bundle divertor [Ref. 44] will be an important component for the STR, for it serves as a conduit for channeling plasma exhaust (including wall-generated impurities) out of the torus and into a magnetic field expander (nozzle) where the perpendicular plasma energy can be converted to directed energy along the nozzle axis. Using several relatively small circular coils, a "bundle" of magnetic field lines can be detached from the periphery of the discharge and guided through an exit port in the torus wall (Fig. 15). The bundle divertor concept has already been operated successfully on the DITE (Diverted Injection Tokamak Experiment) [Ref. 44] using both a diagnostic electron beam to confirm field line channeling and under actual ohmic discharge conditions.

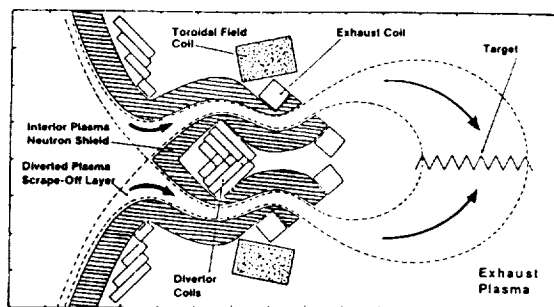


FIGURE 15. - MAIN FEATURES OF A TOKAMAK MAGNETIC BUNDLE DIVERTOR [REF. 44].

Because a typical tokamak discharge consists of a hot interior core, surrounded by a cooler plasma mantle, the volume-averaged density,  $\langle n \rangle$ , and temperature,  $\langle T \rangle$  ( $= \langle nT \rangle / \langle n \rangle$ ), must be used to correctly evaluate the plasma performance. Preliminary estimates [Ref. 43] indicate that a STR burning a 50/50 fuel mixture of spin-polarized DHe<sup>3</sup> could generate ~ 7500 MW of fusion power, ~ 6000 MW of which is transport power and the remainder being bremsstrahlung and synchrotron radiation. The neutron producing DD side reactions are assumed to be suppressed. The major radius, plasma elongation,  $\kappa$ , and aspect ratio for the above example are 2.48m, 3.0, and 2.0, respectively; leading to a plasma volume ( $= 2\pi^2 R_0^2 a \kappa$ ) of 227 m<sup>3</sup>. The toroidal field on axis (at R<sub>0</sub>) and at the center conductor (R<sub>c</sub>) are 8.9 and 10.0 Tesla with paramagnetism accounting for a factor of 2 enhancement in the toroidal field. For a volume-averaged fuel ion density and temperature of  $5 \times 10^{20} / \text{m}^3$  and 50 keV, the fusion power density is ~ 33 MW/m<sup>3</sup> with spin polarization and profile peaking providing a factor of 3 enhancement over that which would be obtained using Eq. (5) alone. Similarly, with profile effects taken into account, the volume-averaged beta value, given by:

$$\langle \beta \rangle B_t^2 = 5 \mu_0 k \langle nT \rangle = 10^{-21} \langle n \rangle \langle T \rangle, \quad (7)$$

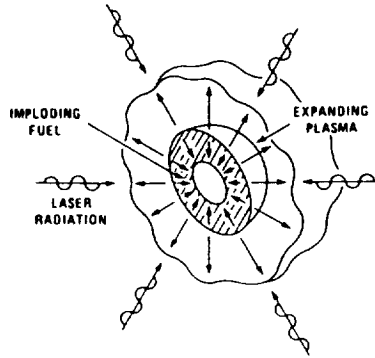
is calculated to be 30%. The overall spacecraft weight is estimated to be ~1033 mT and leads to a specific power of  $\alpha_p = 5.75 \text{ kW/kg}$  (assuming  $P_{\text{jet}} = P_{\text{tr}}$ ).

Lastly, the STR will need very efficient current drive (several amps per watt of sustaining current drive power), due to the large value of plasma current (86 MA) present in the device. It is possible that preferential biasing of "in situ" plasma synchrotron radiation [Ref. 45] and the "bootstrap current effect" caused by radial plasma diffusion [Ref. 46] can drive all or a substantial portion of the required currents in the ST during steady state operation. If such self-generated currents can be realized in future experiments, the power and equipment requirements for current drive can be significantly reduced.

Inertial Confinement Fusion Rocket

In the magnetic confinement concepts discussed above, the fuel must be maintained at fairly low density ( $10^{20} - 10^{21}/m^3$ ) due to  $\beta$  and magnetic field strength limitations. As a result, confinement times of a second or more are required in order to get a substantial burnup of the fuel. In the inertial confinement fusion (ICF) approach [Ref. 47], the requirements on density and confinement times are reversed. Here, multi-megajoule pulses (~10 ns in duration) of photons or ions from a "driver" are used to ablate off the outer surface of a fuel pellet (Fig. 16). Spherical rocket-like reaction forces implode the remaining fuel to stellar densities while simultaneously heating the central core of the pellet to the nuclear

**Implosion of an Inertial Confinement Fusion Target**



Scaling Laws:

$$\left. \begin{aligned} \tau E &= \tau D \sim \frac{R_c}{C_s} \\ n_i &= \rho / \bar{m}_i \end{aligned} \right\} \Rightarrow n \tau E \sim \rho R / \bar{m}_i C_s$$

Energy Balance:

$$E_{fusion} = G \epsilon_D E_{driver} = \frac{G}{\epsilon_D} E_{fuel} (thermal)$$

FIGURE 16. - HIGH FUEL DENSITY ( $\rho$ ), ENERGY GAIN (G), AND COUPLING EFFICIENCY ( $\epsilon_D$ ) ARE NECESSARY COMPONENTS OF INERTIAL CONFINEMENT FUSION.

ignition temperatures (~10 keV). As the fuel burns, the energy generated is used to heat and ignite more fuel. A thermonuclear burn wave driven by  $\alpha$ -particle self heating propagates radially outward through the compressed fuel. Compared to the disassembly time of the pellet ( $\tau_D \sim R_c/C_s$ , with  $R_c$  being the compressed pellet radius and  $C_s$  the ion sound speed), the fuel reacts so rapidly ( $<10^{-12}$  s) that it is confined by its own inertia.

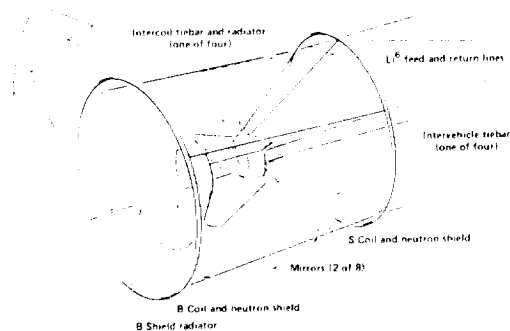
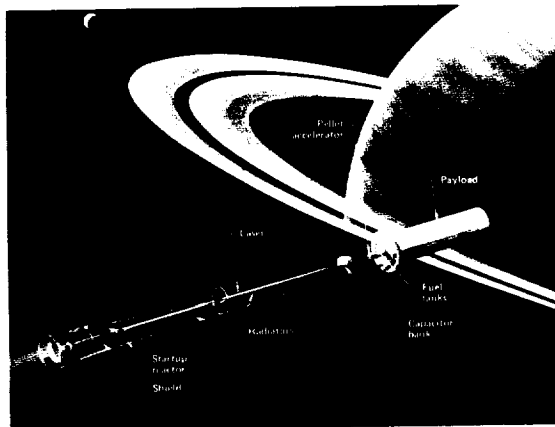
Although magnetic fusion research has been ongoing for the last three decades, the less developed inertial confinement approach offers the possibility of more compact, lower weight propulsion systems. This is due to the absence of heavy superconducting coils in the primary reactor. By exploiting the high repetition rates (10-100 Hz) and gain possibilities of ICF, an inertial fusion rocket (IFR) can operate, in principle, at very high power levels (10 - 100 GW; 1 GW = 1000 MW), which would be extremely difficult if not impossible to achieve with continuous drive magnetic confinement fusion.

For an ICF system to produce usable quantities of fusion power, the initial investment of driver energy ( $E_{\text{driver}}$ ) must be efficiently coupled into the pellet ( $E_{\text{fuel}}/\epsilon_d$ ;  $\epsilon_d$  is the driver energy coupling efficiency) and multiplied during fuel burnup to produce an attractive energy gain ( $G = E_{\text{fusion}}/E_{\text{driver}}$ ). The driver energy that effectively couples to the pellet must (1) isentropically compress [Ref. 48] the fuel load to densities on the order of a  $\text{kg}/\text{cm}^3$ , and (2) ignite the pellet's central core. This energy investment is characteristically quite large -- on the order of several megajoules. Because large driver energies usually correspond to high driver weight, there is a strong incentive to design high gain targets ( $G \sim 1000$ ) that can maximize the fusion power output per pulse. The fuel loading in these pellets is usually quite small, however. In a practical target design the fractional burnup ( $f_b$ ) of the fuel is expected to be ~ 30 to 50% (substantially higher than in magnetic systems). Assuming the use of deuterium fuel (specific energy of 345 MJ/mg), a target yield of ~2000 MJ will require a fuel loading in the compressed pellet of

$$m_c (\text{mg}) = \frac{E_{\text{fusion}} (=2000 \text{ MJ})/345 \text{ MJ/mg}}{f_b (\sim 40\%)} \approx 15 \text{ mg.}$$

Because of the tiny amount of mass involved, the energy release is in the form of a small and potentially manageable explosion. The initiation of a sustained series of these fusion microexplosions within an axially asymmetric magnetic mirror is the essence of inertial fusion rocket propulsion. The thrust of the spacecraft would be produced by redirecting the charged plasma debris from the microexplosion through the larger of the mirror loss cones and out the rear of the vehicle (Fig. 17).

Hyde has performed a detailed analysis [Ref. 49] of an IFR that uses two 2 MJ, 6% efficient high temperature (1000 K) krypton fluoride (KrF) lasers, each operating at 50 Hz, as the driver. With slightly tritium-enriched deuterium as fuel and a high gain target ( $G = 1000$ ), the fusion power output consisted of 1280 MW of charged plasma power



Extraterrestrial Vehicle Thrust Chamber

FIGURE 17. - INERTIAL CONFINEMENT FUSION ROCKETS CAPABLE OF HIGHER SPECIFIC POWER AND IMPULSE OPERATION THAN THEIR MAGNETIC COUNTERPARTS COULD MAKE RAPID SOLAR-SYSTEM-WIDE TRAVEL FEASIBLE. (COURTESY OF LAWRENCE LIVERMORE NATIONAL LABORATORY).

[consistent with the 60% charged particle fraction of the cat-DD fuel cycle] and 710 MW in the form of x-ray and neutron radiation. Additional propellant mass (~10 times the fuel loading) surrounds the pellet providing the ablative material and also augmenting the engine's propulsive thrust. The exhaust velocity ( $v_{ex}$ ) and jet power are given by

$$v_{ex} = gIsp = \eta_j (2E_{cp}/m_p)^{1/2} \quad (8)$$

and

$$P_{jet} = 1/2 m_p \nu v_{ex}^2 = \eta_j^2 \nu E_{cp} \quad (9)$$

where  $\eta_j^2$  is the efficiency of the magnetic nozzle in converting charged particle fusion power ( $\nu E_{cp}$ ) to jet power,  $m_p$  is the initial pellet mass ( $10 \times m_c$ ), and  $\nu$  is pellet rep rate. With  $\nu = 100$  Hz and  $\eta_j = 65\%$ , the exhaust velocity and jet power are estimated to be 2650 km/s ( $Isp = 270$  kiloseconds) and 53 GW. The corresponding thrust level ( $F = m_p \nu v_{ex}$ ) is ~ 40 kN. The total weight of the engine system was estimated to be 486 mT, 54% of which is attributed to the drive system and 34% to the magnetic thrust chamber. Based on the above parameters, the specific power of the IFR is  $\alpha_p = 100$  kW/kg.

## Mission Performance Characteristics

Manned expeditions to Mars have been studied extensively in the past using a variety of propulsion concepts. Traditionally, propulsion systems have been characterized as either high thrust "specific impulse-limited systems" (such as chemical and solid core nuclear thermal rockets) or low thrust "power-limited systems" (such as nuclear electric rockets). The gas core engines discussed above represent a hybrid configuration capable of high thrust operation and Isp levels comparable to several of today's EP concepts. The GCR remains Isp-limited (<7000s), however, because of constraints imposed by excessive structural and nozzle heating. The fusion systems provide a unique third category of engine capable of high thrust/high Isp operation and fast interplanetary travel throughout the Solar System. The performance of these direct thrust nuclear engines is discussed below.

### Fission Systems

One of the original objectives of NASA's NERVA program was to develop a nuclear rocket engine that could form the basis for a modular nuclear transportation stage. This stage was to function as a "space propulsion workhorse" for the high  $\Delta V$  missions contemplated by NASA, such as a manned Mars mission. In early mission studies reusability was not a high priority and emphasis was placed principally on identifying an optimum thrust engine/propulsion module [Ref. 24] offering multimission capability. By clustering engines or propulsion modules, individual stages could be assembled that had a near optimum thrust-to-weight ratio for each propulsion stage or mission phase (for example, the optimum ratio for the Earth departure stage is almost constant at about 0.2 [Ref. 50]). Because each discrete stage was jettisoned after limited use, the full propulsive capability of the nuclear engine was significantly underutilized.

By providing for propellant transfer between adjoining stages (a concept referred to as "active vampire" [Ref. 51]), the duration of each propulsive stage was no longer limited by the propellant capacity of the stage, but rather by the operational lifetime of the engine. As the lifetime of the solid core fuel elements increased from 1 hour to more than 10 hours, emphasis shifted to a reusable engine scenario where a nuclear stage could be restarted to provide all or part of the total incremental velocity ( $\Delta V$ ) required for the mission. Werner von Braun employed the reusable engine concept in describing NASA's plans for a proposed manned Mars expedition at a hearing of the Senate Committee on Aeronautical and Space Science [Ref. 52]. The mission would be accomplished using two spacecraft, each carrying a 6-man crew and having an initial mass in Earth orbit (IMEO) of 727 mT (~1.6 million pounds). Each spaceship would use three 445 kN (100,000 lbf) NERVA type engines (Isp~850 s) of which two would be used only for Earth orbital departure. Assembled in low Earth orbit (555 km), the ships would be moving at ~7.6 km/s and require only an additional 3.6 km/s to reach Earth escape velocity and depart on a minimum energy trajectory (~ 270 day trip) to Mars. After the trans-Mars insertion burn, the two strap-on boosters would separate and return to Earth for liquid hydrogen refueling and reuse. Subsequent mission maneuvers (Mars capture and escape, and Earth capture) were accomplished using

the remaining NERVA engine. The total mission duration (including a Venus swingby on the return leg of the mission) was 720 days with 80 days on the Martian surface. What was most impressive about von Braun's proposed mission scenario using solid core engines was the fact that the returned payload mass fraction for each ship (consisting of the NERVA boosters plus the core spaceship) was ~22% (excluding the 100 mT left at Mars).

Manned Mars Missions (MMMs) are again being contemplated by NASA [Ref. 53] and a variety of propulsion systems are being examined. Next to chemical propulsion, the SCR is the only other concept that has been experimentally demonstrated at the thrust and power levels required for a MMM. The performance characteristics of several high thrust propulsion concepts are shown in Table 5. A 1999 opposition class Mars mission is selected for comparing the near term chemical and SCR technologies. The mission profile includes a 360 day outbound

Table 5  
Comparison of Chemical, Solid- and Gas-Core Rockets  
for Manned Mars Missions

<u>Parameters</u>	1999 Opposition Class Mission*		
	Chemical (LO <sub>2</sub> /LH <sub>2</sub> )	SCR <sup>a</sup>	GCR <sup>b</sup>
I <sub>sp</sub> (s)	460	825	5000
τ <sub>RT</sub> (days)	680	680	200
M <sub>p</sub> (mT)	1440 (550) <sup>c</sup>	522 (209)	350
M <sub>i</sub> (mT)	1623 (714)	755 (420)	770
M <sub>p</sub> /M <sub>i</sub> (%)	88.7 (77.0)	69.1 (49.8)	45.5
<u>Launch Requirements: No. Flights and Cost</u>			
STS (30)/HLLV (120) <sup>d</sup>	54/16 (24/6)	25/6 (14/4)	7
5k\$/kg/1.25k\$/kg	8.1B\$/2.0B\$ (3.6B\$/0.9B\$)	3.8B\$/0.9B\$ (2.1B\$/0.5B\$)	-1B\$

\* ΔV = 12.5 km/s: TMI(4.43), MOI(2.76), TEI(1.62), EOI(3.72)

<sup>a</sup> Three 440 kN (10<sup>5</sup> lbf) engines provide a F/W<sub>i</sub> ~0.2

<sup>b</sup> One 22 kN (5000 lbf) engine provides a F/W<sub>i</sub> of ~3x10<sup>-3</sup>

<sup>c</sup> Numbers in parenthesis assume aerobraking at Mars and Earth

<sup>d</sup> Assumed tonnage delivered into LEO

33

leg with Venus swingby<sup>\*</sup>, a 60 day surface stay, and a 260 day return leg. To complete this mission the chemical system requires an initial mass in Earth orbit ( $M_i$ ) of 1623 mT. The propellant mass fraction ( $M_p/M_i$ ) is ~ 89%. By using aerobraking to dissipate the spacecraft's incoming kinetic energy at Mars and Earth, the IMEO for the chemical system can be reduced by ~60% (to ~ 714 mT). While attractive from a weight standpoint, the principal uncertainty with aerobraking manned vehicles is the ability of the crew to function in a severe g-load environment after prolonged periods in zero gravity. Earth aerobraking for certain opposition class missions can be particularly severe and may require some propulsive braking to decrease the entry velocity and reduce the g-loads to levels that can be safety tolerated by the crew.

By contrast, the SCR, with its higher Isp and lower propellant mass fraction, can perform the entire mission propulsively and with an IMEO that is within 6% of the aerobraked chemical system. Further reductions in initial weight may also be possible for the SCR once a highly reliable, man-rated aerobraking capability has been demonstrated for use at Earth and Mars. With propellant loadings comparable to that of the all propulsive chemical system, the SCR can transport larger payloads to Mars or can travel higher  $\Delta V$  trajectories resulting in shorter trip times. Direct nuclear propulsion can also provide a significant savings in both the number and cost of Earth-to-orbit launches required for spacecraft assembly. Compared to the SCR system, an all propulsive chemical mission requires 29 additional shuttle flights to ferry the mass difference into orbit. At ~0.15B\$ per launch (~5k\$/kg assuming a 30 mT cargo capacity), this difference amounts to an additional 4.3B\$ per mission. If multiple missions are envisioned, as would be the case if a Mars outpost or base is to be established, then the savings accrued through the use of the SCR could pay for its final development phase several times over. Even assuming the development of a Saturn V class (~120 mT capacity) Heavy Lift Launch Vehicle (HLLV), to improve the logistics and cost associated with orbital assembly, the SCR still maintains a factor of 2 edge over the chemical system in the launch requirements area.

With its high thrust/high Isp features, the radiator-cooled GCR is capable of performing a wide range of MMMs ranging from quick "courier-type" shuttle missions to the more demanding science/exploration mission. The 5000 s GCR shown in Table 5 can deposit 150 mT at Mars and return 100 mT to Earth with a roundtrip time of ~200 days [Ref. 36]. This is twice as much payload as assumed for the chemical and SCR systems. The optimum thrust for this 5000 s engine is 22 kN and the reactor power is only 750 MW--half that planned for NERVA flight engine. The propellant mass fraction is also quite attractive being less than 50%.

---

\* An outbound Venus swingby allows the spacecraft to arrive at Mars ahead of Earth and permits a low-energy return leg to Earth. Von Braun's scenario assumed an inbound Venus flyby to slow down the spacecraft on its return to Earth.

By increasing the propellant loading higher  $\Delta V$  missions are possible and exceedingly short trip times become feasible. Figure 18 compares IMEO for several advanced nuclear propulsion concepts as a function of

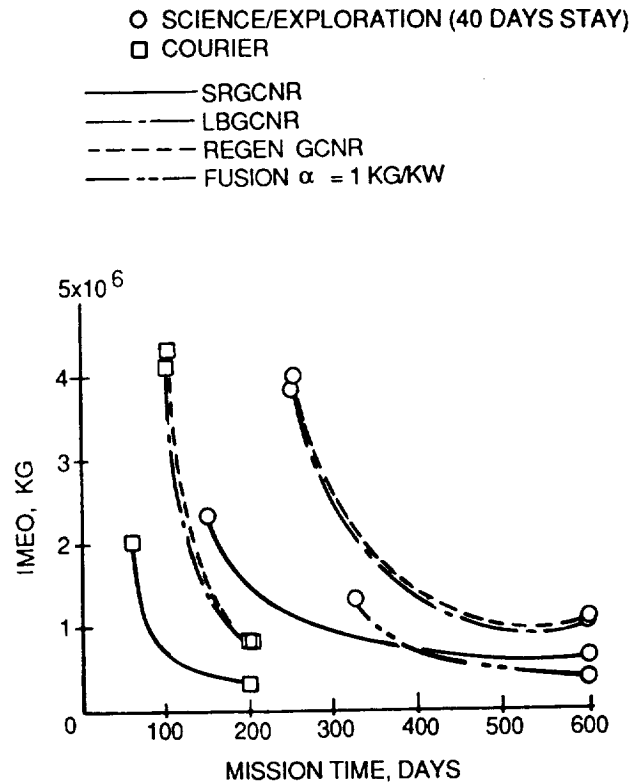


FIGURE 18. - SENSITIVITY OF IMEO WITH MARS ROUND TRIP MISSION TIME FOR VARIOUS ADVANCED NUCLEAR ROCKET ENGINES (REF. 54).

Mars roundtrip time and mission type [Ref. 54]. Included are the light-bulb, regeneratively-and radiator-cooled GCRs, and a fusion engine with an assumed specific power of 1 kW/kg. The courier mission carries no inert payload to the planet and uses a reentry vehicle and atmospheric braking to return the crew to Earth. In the science exploration mission a 150 mT payload is left at Mars during a 40 day surface stay and an additional 100 mT is propulsively returned to Earth orbit on board a core spacecraft shown in Fig. 19.

Figure 18 shows that for an IMEO of ~2000 mT, 60 day courier missions to Mars are possible using the radiator-cooled GCR. Propellant mass and tankage comprise 90% of this weight while the engine-related hardware (the GCR and its uranium storage and supply system) accounts for another 6.5%. The remaining mass is attributed to the manned mission module and reentry vehicle. The GCR engine used in this mission produces ~8500 MW of thermal power and generates 220 kN of thrust at an Isp of ~5700 s. By extending the trip time to 80 days the IMEO can be cut in half to ~1000 mT. The same engine can also perform exploration missions of 160 and 280 days total duration with IMEOs of 2000 and 1000 mT, respectively.

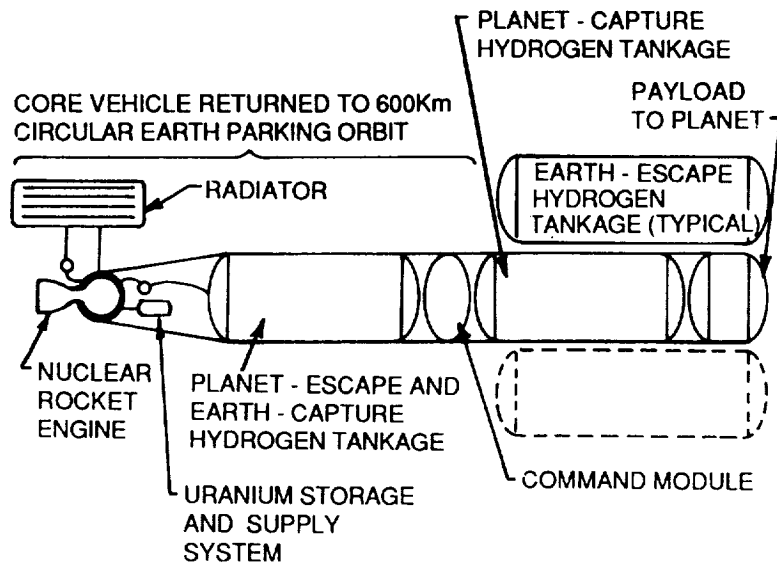


FIGURE 19. - SCHEMATIC OF REUSABLE, RADIATOR-COOLED GCR SPACECRAFT USED IN MANNED MARS MISSION ANALYSIS (REF. 54).

The nuclear light bulb and regeneratively-cooled GCRs also have impressive capabilities compared to the SCR, however, their competitiveness with the radiator-cooled GCR is hampered by the limited Isp (~ 2500 s) of these engine concepts. Only the fusion engine is capable of outperforming the radiator-cooled GCR for the Mars exploration mission and this advantage exists only if trip times in excess of 1 year are specified. For trips to the outer Solar System, the high Isp capability of the fusion engine (> 10<sup>5</sup>s) makes it a propulsion system without equal. With high specific power systems ( $\alpha \sim 5\text{-}100 \text{ kW/kg}$ ), true Solar System class spaceships can be considered.

### Fusion Systems

High power fusion rockets possess the best attributes of both fission thermal engines (prolonged operation at relatively high thrust) and the fission-powered electric propulsion systems (high Isp). It is envisioned that the fusion spacecraft would depart from and return to geosynchronous Earth orbit. In traveling between planetary bodies the Sun is considered to be the only source of gravitational force. Because the initial acceleration levels for the fusion systems examined range from 3 to 5 milligees, (compared to the Sun's gravitational pull of 0.6 milligees), straight line trajectories have been assumed. To illustrate the performance potential for the fusion systems we have considered "1 way" and "roundtrip" continuous burn acceleration /deceleration trajectory profiles which assume constant Isp, F and P<sub>jet</sub> operation. The equations describing the transit times for the outbound and return legs of a journey from A to B (and back again) along with the distances traveled are given by [Ref. 43]:

$$\tau_{AB}(s) = \frac{Isp(s)}{F/W_f} \left(\frac{1}{\beta}\right) \left(\frac{1}{\alpha} - 1\right) \quad (10)$$

$$\tau_{BA}(s) = \frac{I_{sp}(s)}{F/W_f} \left( \frac{1}{\beta} - 1 \right) \quad (11)$$

$$\tau_{RT}(s) = \tau_{AB} + \tau_{BA} = \frac{I_{sp}(s)}{F/W_f} \left( \frac{1}{\alpha\beta} - 1 \right) \quad (12)$$

$$D_{AB}(m) = \frac{g I_{sp}^2}{F/W_f} \left( \frac{1}{\beta} \right) \left( \frac{1}{\sqrt{\alpha}} - 1 \right)^2 = D_{BA}(m) \quad (13)$$

$$D_{BA}(m) = \frac{g I_{sp}^2}{F/W_f} \left( \frac{1}{\sqrt{\beta}} - 1 \right)^2 \quad (14)$$

where  $W_f = M_f g$  is the dry weight,  $1/\alpha = M_i/M_B$  ( $M_B = M_f + M^{B \rightarrow A}$ ;  $M^{B \rightarrow A}$  being the propellant used in traveling from B to A),  $1/\beta = M_B^P/M_f^P$  and  $R_M = 1/(\alpha\beta)$ . By specifying a particular planetary mission and its distance from Earth, Eqs. (13) and (14) can be used to determine  $1/\alpha$  and  $1/\beta$  and their product, the spacecraft mass ratio. By knowing the mass of the thrust producing system ( $M_W$ ) and specifying a payload mass ( $M_L$ ), the IMEO, propellant requirements and trip times can be calculated. Assuming a planetary refueling capability, Eqs. (11) and (14) can be used to calculate "1 way" results. In this case  $R_M = 1/\beta$ .

The performance characteristics for the STR and IFR are summarized in Tables 6 and 7. Table 6 indicates that with planetary refueling, the STR can journey to Mars in ~ 34 days. The IMEO is 2135 mT of which 42% is propellant, 9.4% is payload and 48% is engine. The initial acceleration level is ~3 milligees which is 5 times the value of the

Table 6  
Spherical Torus Fusion Rocket Performance

STR Characteristics							
Polarized DHe <sup>3</sup> , $I_{sp} = 20ks$ , $\dot{m}_p = 0.308$ kg/s, $\alpha_p = 5.75$ kW/kg, $M_W = 1033$ mT, $M_L = 200$ mT							
1 Way "Continuous Burn/Constant $I_{sp}$ " Trajectory Profile							
Mission*	$D_{AB}$ (A.U.)	$R_M$	$M_i$ (mT)	$M_p$ (mT)	$M_L/M_i$ (%)	$\tau_{AB}$ (days)	$a_i$ ( $10^{-3} g_0$ )
Mars	0.524	1.732	2135	902	9.4	33.9	~ 2.9
Ceres	1.767	2.497	3079	1846	6.5	69.4	2.0
Jupiter	4.203	3.590	4427	3194	4.5	120.0	~ 1.4

"Round Trip" Trajectory Results								
Mission*	$R_M (= \frac{1}{\alpha\beta})$	A-B $M_p$	B-A $M_p$	A-A $M_p$	$M_i$	$\tau_{AB}$	$\tau_{BA}$	$\tau_{RT}$
Mars	2.664	1149	902	2051	3284	43.2	33.9	77.1
Ceres	4.667	2675	1846	4521	5754	100.5	69.4	169.9
Jupiter	7.783	5169	3194	8363	9596	194.3	120.0	314.3

\*Closest approach distances to Earth.

Table 7  
 Inertial Fusion Rocket Performance  
 IFR Characteristics

Cat-00, $I_{sp} = 270\text{ks}$ , $\dot{m}_p = 0.015 \text{ kg/s}$ , $\alpha_p = 110\text{kW/kg}$ , $M_W = 486\text{mT}$ , $M_L = 200\text{mT}$							
Round Trip "Continuous Burn/Constant $I_{sp}$ " Trajectory Profile							
Mission*	$D_{AB}$ (A.U.)	$R_M (= \frac{1}{\alpha_B})$	$M_i$ (mT)	$M_p^{A-A}$ (mT)	$M_L/M_i(\%)^+$	$\tau_{AB}$ (days)	$\tau_{RT}$ (days)
Mars	0.524	1.104	757.3	71.3	26.4	27.7	55.0
Ceres	1.767	1.196	820.5	134.5	24.4	53.1	103.7
Jupiter	4.203	1.309	898	212.0	22.3	84.6	163.6
Saturn	8.539	1.453	997	311.0	20.1	125.5	239.8
Uranus	18.182	1.689	1159	473.0	17.3	194.1	364.7
Neptune	29.058	1.901	1304	618.0	15.3	257.3	476.9
Pluto	38.518	2.063	1415	729.0	14.1	306.6	562.7

\*Closest approach distances to Earth.  
 +For outboard leg of journey.

Sun's gravitational pull at Earth. Jupiter can also be reached in ~ 4 months with a propellant loading of 3200 mT. Without a planetary refueling capability, the spacecraft must carry along sufficient propellant for the return trip. This requirement increases the overall IMEO and duration of the Jupiter mission to 9600 mT and 10.3 months, respectively. In all of the results shown, it is assumed that an equivalent amount of payload is returned for each mission. While the cost of launching the hydrogen propellant for a round trip Jupiter mission would be large (~ 8.4B\$ assuming 1k\$/kg for an advanced launch system of the 21st century), the STR could bring to Earth an extremely valuable cargo - He<sub>3</sub> from Jupiter. At today's current price of 0.7B\$/kg [Ref. 11], 200 mT of He<sub>3</sub> would be worth 140B\$ - a good return on investment.

The STR results shown in Table 6 assumed the use of spin-polarized DHe<sub>3</sub> in order to eliminate neutron radiation and obtain a lighter spacecraft. If the benefits of spin-polarized DHe<sub>3</sub> are not achievable, low-neutron-yield magnetic fusion engines could still be possible by running a lean D, rich He<sub>3</sub> fuel mixture to suppress neutron production. A penalty in engine performance would result, however, due to a reduced fusion power output and an increase in shield mass. Fuel costs would also be expected to rise due to the low fractional burnup of most MCF concepts (<10%) and the loss of costly He<sub>3</sub>.

With the possibilities for high rep rate drivers and high  $\rho R$  (~10 - 20g/cm<sup>2</sup>)/high gain (G~1000) target designs, the IFR can not only burn abundant deuterium fuel efficiently (~5 to 10 times better than MCF systems), but it can do so with a relatively lightweight engine system (<500 mT) [see Table 7]. And while MCF rockets can reach out into the Solar System by employing planetary refueling, the IFR can perform roundtrip missions to Pluto (carrying a 200 mT payload) in less than

20 months (no refueling required). The IMEO would be 1415 mT with propellant and payload mass fractions of ~ 52% and 14%, respectively. We know of no other advanced propulsion concept with this capability. Small quantities of tritium would be bred on-board the spacecraft to facilitate ignition of the DD fuel pellets and the deuterium fuel load that comprises ~ 10% of the propellant inventory would cost ~ 73 M\$ at current prices of ~1k\$/kg.

Orth has examined the characteristics of a DT-fueled IFR capable of performing 100 day roundtrip missions to Mars with 10 day stay times and a 100 mT payload [Ref. 55]. The spacecraft's IMEO is 5800 mT of which 4100 mT is propellant mass and 40 mT is DT fuel (with 25 mT of tritium carried on board). With a high gain target design (G-1500) and a rep rate of 30 Hz, the engine generates a total power output of 225,000 MW of which only 9% (20,280 MW) is available as jet power. The engine thrust and Isp are 245 kN (~54,000 lbf) and ~20 ks, respectively. The above parameters highlight the drawbacks of using DT fuel; a large wasted power component (which also represents a major radiation hazard), and reduced Isp (a result of adding significant propellant mass around the DT pellet to improve the plasma debris fraction). The tritium fuel costs for such a mission are also expected to be prohibitive: 187.5B\$ at current tritium prices of 7.5M\$/kg [Ref. 11]. With such performance characteristics, a DT-fueled IFR will not be competitive with other advanced propulsion concepts expected to be available in the 2025 time frame, such as the GCR. In order for the IFR to realize its ultimate potential as a true "Solar System class" engine, attention must be focussed on the development of efficient, multimegajoule, high rep rate drivers and on high  $\rho R$ /high gain target designs that will enable cheap and abundant deuterium fuel to be burned effectively.

### Summary and Conclusions

Convenient interplanetary travel will require the development of advanced nuclear propulsion systems with large  $\alpha_p$  and Isp capability. While there is considerable interest in low thrust nuclear-electric propulsion systems at present, high thrust analogues for ET, EM and ESI systems also exist in the form of SCR, GCR, and fusion rocket systems. In the case of the SCR, the concept has been extensively tested and the thrust and power levels required for MMMs have been demonstrated. What remains to be done is to build and test an actual flight engine the designs for which already exist. The factor of two advantage in Isp over chemical rockets allows the SCR to perform a variety of missions in near Earth, cislunar, and interplanetary space with lower IMEO and mission cost. With increased propellant loadings, faster, higher  $\Delta V$  transfer orbits can also be traveled resulting in shorter trip times. The SCR can therefore provide a more robust space transportation system.

Beyond the SCR, the nuclear light bulb and radiator-cooled, open cycle GCRs can provide a factor 5 improvement in Isp over the SCR. The nuclear light bulb concept offers the potential for perfect containment of fission products and efficient fuel burnup through the use of a transparent wall structure and a closed fuel processing system. The porous wall, open cycle GCR uses fluid mechanical means

for separating the gaseous fuel and propellant. While a small percentage (<1%) of fuel is exhausted along with the propellant, the absence of wall structure allows the radiator-cooled versions of this engine to operate at considerably higher values of specific impulse-- in the range of 3000-7000 s. With a specific power and impulse potential of ~50 kW/kg and 5000 s, respectively, quick courier trips to Mars (of ~80 days) or longer duration exploration/cargo missions (lasting ~280 days) are possible with IMEOs of ~1000 mT. Key operational features of both the light bulb and open cycle engine concepts have already been demonstrated experimentally in single and combined experiments using heated uranium plasmas sources to simulate the actual engine. Awaiting development, however, are important nuclear tests at both the sub- and full-scale engine levels.

Following demonstrations of energy breakeven in the late 1980's and ignition in the 90's, the 21st century will see the development of fusion propulsion systems based on high power density magnetic and inertial confinement fusion concepts. Magnetic fusion engines with specific powers in the range of 2.5 to 10 kW/kg and Isp's of ~20,000 s will be capable of transporting 200 mT cargos to and from Mars during 80 day roundtrip missions.

By employing planetary refueling at selected locations (e.g., Mars, Callisto and Titan), these engines will allow man to extend his sphere of influence beyond Mars into the outer Solar System. With the development of inertial fusion rockets will arrive the era of the true Solar System class spaceship. Possessing specific powers and impulses of ~100 kW/kg and 200-300 kiloseconds, IFRs will offer outstandingly good performance over a wide range of interplanetary destinations and roundtrip times. Even Pluto will be accessible with roundtrip times of less than 2 years and IMEO's of ~1500 mTs.

The promise of the IFR will not be realized overnight, however, but will emerge from the development of increasingly more efficient nuclear propulsion systems. The solid core fission thermal rocket represents the first vital link in this evolutionary chain. It can provide this country with a high thrust propulsive capability far more advanced than any other system currently available or anticipated in the relatively near future. With early implementation, for near Earth and cislunar missions, valuable operational experience can be also gained that will be important to future manned planetary expeditions. Beyond the SCR a succession of advanced nuclear engines will follow, each generation reaching higher levels of specific power and impulse and culminating in the IFR that will open the entire Solar System to manned exploration and colonization.

#### REFERENCES

1. S. J. Adelman and B. Adelman, Bound for the Stars, Prentice-Hall, Inc., Englewood Cliffs, New Jersey, 1981, pp. 133-141.

2. D. R. Koenig, "Experience Gained from the Space Nuclear Rocket Program (Rover)," LA-10062-H, Los Alamos National Laboratory, Los Alamos, New Mexico, May 1986.
3. H. Ludewig, A. J. Manning, and C. J. Raseman, "Feasibility of Rotating Fluidized Bed Reactor for Rocket Propulsion," J. Spacecraft, Vol. 11, Feb. 1974, p. 65.
4. R. G. Ragsdale, "To Mars in 30 Days by Gas-Core Nuclear Rocket," Astronautics and Aeronautics, Jan. 1972, p. 65.
5. J. L. Hilton, J. S. Luce, and A. S. Thompson, "Hypothetical Fusion Propulsion Rocket Vehicle," J. Spacecraft, Vol. 1, May-June 1964, p. 276.
6. K. Boyer and J. D. Balcomb, "System Studies of Fusion-Powered Pulsed Propulsion Systems," AIAA 71-636, June 1971.
7. D. M. North, "USAF Focuses Development on Emerging Technologies," Aviation Week and Space Technology, Feb. 24, 1986, p. 19.
8. J. R. Powell, H. Ludewig, F. L. Horn, et. al., "Nuclear Propulsion System for Orbit Transfer Based on the Particle Bed Reactor," Transactions of the Fourth Symposium on Space Nuclear Power Systems, CONF-870102-SUMMS., Albuquerque, New Mexico, Jan. 12-16, 1987, pp. 73-76.
9. R. L. Forward, B. N. Cassenti, and D. Miller, "Cost Comparisons of Chemical and Antihydrogen Propulsion Systems for High  $\Delta V$  Missions," AIAA 85-1455, July 1985.
10. J. R. Lamarsh, Introduction to Nuclear Reactor Theory, Addison-Wesley Publishing Company, Inc., Reading, MA, 1966, pp. 86-104.
11. J. Rand McNally, Jr., "Physics of Fusion Fuel Cycles," Nuclear Technology/Fusion, Vol. 2, Jan. 1982, p. 9.
12. L. J. Wittenberg, J. F. Santarius, and G. L. Kulcinski, "Lunar Source of He<sup>3</sup> for Commercial Fusion Power," Fusion Technology, Vol. 10, Sept. 1986, p. 167.
13. R. M. Kulsrud, H. P. Furth, E. J. Valeo, and M. Goldhaber, "Fusion Reactor Plasmas with Polarized Nuclei," Phys. Rev. Letters, Vol. 49, p. 1248.
14. B. P. Adyasevich and D. E. Fomenko, "Analysis of Investigation of the Reaction D(d,p)T with Polarized Deuterons," Sov. J. Nucl. Phys., Vol. 9, 1969, p. 167.
15. B. W. Knight, B. B. McInteer, R. M. Potter, and E. S. Robinson, "A Metal Dumbo Rocket Reactor," LA-2091-del, Los Alamos Scientific Laboratory, Los Alamos, New Mexico, May 1957.
16. F. E. Rom, "Advanced Reactor Concepts for Nuclear Propulsion," Astronautics, Oct. 1959, p. 20.

17. R. W. Schroeder, "NERVA - Entering a New Phase," Astronautics and Aeronautics, May 1968, p. 42.
18. J. R. Powell and T. E. Botts, "Particle Bed Reactors for Space Power and Propulsion," in Orbit Raising and Maneuvering Propulsion: Research Status and Needs, ed., L. H. Gaveny, Progress in Astronautics and Aeronautics Series, Vol. 89, 1984, p. 495.
19. D. Buden, "Operational Characteristics of Nuclear Rockets," J. Spacecraft, Vol. 7, July 1970, p. 832.
20. J. H. Altseimer, G. F. Mader, and J. J. Stewart, "Operating Characteristics and Requirements for the NERVA Flight Engine," J. Spacecraft, Vol. 8, July 1971, p. 766.
21. J. H. Beveridge, "Feasibility of Using a Nuclear Rocket Engine for Electrical Power Generation," AIAA 71-639, June 1971.
22. W. Y. Jordan, Jr., R. J. Harris, and D. R. Saxton, "Toward Modular Nuclear-Rocket Systems," Astronautics and Aeronautics, June 1965, p. 48.
23. R. R. Holman, Westinghouse Advanced Energy Systems Division, Personal communication.
24. W. E. Durkee and F. B. Damerval, "Nuclear Rocket Experimental Engine Test Results," J. Spacecraft, Vol. 7, Dec. 1970, p. 1397.
25. R. R. Holman and B. L. Pierce, "Development of NERVA Reactor for Space Nuclear Propulsion," AIAA 86-1582, June 1986.
26. R. G. Ragsdale and E. A. Willis, Jr., "Gas-Core Rocket Reactors A New Look," AIAA 71-641, June 1971.
27. R. V. Meghreblian and H. J. Stumpf, "Gaseous Core Reactors," Proc. 3rd Symp. on Advanced Propulsion Concepts, Cincinnati, OH, Oct. 2-4, 1962, pp. 293-339.
28. R. G. Ragsdale, "High Specific Impulse Gas Core Reactors," NASA TM X-2243, NASA/Lewis Research Center, Cleveland, OH, March 1971.
29. L. H. Fishbach, "Mission Performance Potential of Regeneratively Cooled Gas-Core Nuclear Rockets," NASA TM X-2256, NASA/Lewis Research Center, Cleveland, OH, April 1971.
30. E. P. Coomes, et. al., "PEGASUS: A Multi-Megawatt Nuclear Electric Propulsion System," AIAA 86-1583, June 1986.
31. J. S. Kendall and T. S. Latham, "Summary of Fluid Mechanics and Engine Characteristics Research on the Nuclear Light Bulb Engine Concept," AIAA 70-689, June 1970.
32. T. S. Latham, "Summary of the Performance Characteristics of the Nuclear Light Bulb Engine," AIAA 71-642, June 1971.

33. J. F. Kunze, G. D. Pincock and R. E. Hyland, "Cavity Reactor Critical Experiments," Nuclear Applications, Vol. 6, Feb. 1969, pp. 104-115.
34. J. H. Lofthouse and J. F. Kunze, "Spherical Gas-Core Reactor Critical Experiment," NASA CR-72781, 1971.
35. D. M. Barton, et. al., "Plasma Core Reactor Experiments," Paper 3D-13, 1977 IEEE International Conference on Plasma Science, 1977.
36. R. G. Ragsdale, "Status of Open-Cycle Gas Core Reactor Project Through 1970," NASA TM X-2259, NASA/Lewis Research Center, Cleveland, OH, March 1971.
37. G. H. McLafferty, "Gas Core Nuclear Rocket Engine Technology Status," J. Spacecraft, Vol. 7, Dec. 1970, p. 1391.
38. J. R. Williams, et. al., "Fluid Dynamics of Spherical Cavity Reactors," Transactions of the Fourth Symp. on Space Nuclear Power Systems, CONF-870102-SUMMS., Albuquerque, New Mexico, Jan. 12-16, 1987, pp. 153-155.
39. Y-K. M. Peng, D. J. Strickler, S. K. Borowski, et. al., "Spherical Torus: An Approach to Compact Fusion at Low Field-Initial Ignition Assessments," ANS 6th Top Mtg. on Tech. of Fusion Energy, San Francisco, CA, Mar. 1985.
40. S. Bernabei, et. al., "Lower Hybrid Current Drive in the PLT Tokamak," Phys. Rev. Letters, Vol. 49, 1982, p. 1255.
41. R. J. Goldston, "Progress Toward Breakeven on the Tokamak Fusion Test Reactor," Physics Today, Jan. 1987, p. S-59.
42. M. Porkolab et al., "Lower Hybrid Experiments at the 1 MW Level on ALCATOR-C: Heating and Current Drive," in Proc. 4th Symp. on Heating in Toroidal Plasmas, Rome, Italy, CONF-840311, March 21-28, 1984.
43. S. K. Borowski, "A Physics/Engineering Assessment of a Tokamak-Based Magnetic Fusion Rocket," AIAA 86-1759, June 1986.
44. P. E. Stott, C. M. Wilson, and A. Gibson, "The Bundle Divertor," Nucl. Fusion, Vol. 17, 1977, p. 481, and Nucl. Fusion, Vol. 18, 1978, p. 475.
45. J. M. Dawson and P. K. Kaw, "Current Maintenance in Tokamaks by Use of Synchrotron Radiation," Phys. Rev. Letters, Vol. 48, 1982, p. 1730.
46. R. J. Bickerton, J. W. Connor, and J. B. Taylor, "Diffusion Driven Plasma Currents and Bootstrap Tokamak," Nature, Vol. 229, 1971, p. 110.
47. J. J. Duderstadt and G. A. Moses, Inertial Confinement Fusion, John Wiley and Sons Publishers, New York, 1982.

48. J. Nuckolls, L. Wood, A. Thiessen and G. Zimmerman, "Laser Compression of Matter to Super-High Densities: Thermonuclear (CTR) Applications," Nature, Vol. 239, 1972, p. 139.
49. R. Hyde, "A Laser Fusion Rocket for Interplanetary Propulsion," IAF 83-396, 34th International Astronautical Conference, Budapest, Oct. 1983.
50. P. G. Johnson, "Beyond Apollo with Nuclear Propulsion," Astronautics and Aeronautics, Dec. 1964. p. 22.
51. S. Gronich, R. J. Holl, and K. P. Johnson, "Nonintegral Burn of Nuclear Rockets - An Approach to Low-Cost Space Exploration," J. Spacecraft, Vol. 6, June 1969, p. 723.
52. Statement by Dr. Werner von Braun, Director, Marshall Space Flight Center, Future NASA Space Programs, Hearing of the Senate Aeronautics and Space Science Committee, August 5, 1969, pp. 14-30, 91st Congress, First Session.
53. Manned Mars Missions: A Working Group Report, ed. by M. B. Duke and P. W. Keaton, NASA Report M001, May 1986.
54. L. H. Fishback and E. A. Willis, "Performance Potential of Gas-Core and Fusion Rockets: A Mission Applications Survey," 2nd Symp. on Uranium Plasmas: Research and Applications, AIAA, New York, 1971.
55. C. D. Orth et al., "Transport Vehicle for Manned Mars Mission Powered by Inertial Confinement Fusion", AIAA 87-1904, June 1987.

1. Report No. NASA TM-101354		2. Government Accession No.		3. Recipient's Catalog No.	
4. Title and Subtitle Nuclear Propulsion—A Vital Technology for the Exploration of Mars and the Planets Beyond				5. Report Date	
				6. Performing Organization Code	
7. Author(s) Stanley K. Borowski				8. Performing Organization Report No. E-4369	
				10. Work Unit No. 906-85-44	
9. Performing Organization Name and Address National Aeronautics and Space Administration Lewis Research Center Cleveland, Ohio 44135-3191				11. Contract or Grant No.	
				13. Type of Report and Period Covered Technical Memorandum	
12. Sponsoring Agency Name and Address National Aeronautics and Space Administration Washington, D.C. 20546-0001				14. Sponsoring Agency Code	
15. Supplementary Notes Prepared for Case for Mars III, cosponsored by the American Astronautical Society, Jet Propulsion Laboratory, Los Alamos Laboratory, Ames Research Center, Lyndon B. Johnson Space Center, George C. Marshall Space Flight Center, and the Planetary Society, Boulder, Colorado, July 18-22, 1987.					
16. Abstract The physics and technology issues, and performance potential of various direct thrust fission and fusion propulsion concepts are examined. Next to chemical propulsion the solid core fission thermal rocket (SCR) is the only other concept to be experimentally tested at the power (~1.5 to 5.0 GW) and thrust levels (~0.33 to 1.11 MN) required for manned Mars missions. With a specific impulse of ~850 s, the SCR can perform various near-Earth, cislunar and interplanetary missions with lower mass and cost requirements than its chemical counterpart. Beyond the SCR, a succession of advanced nuclear engines can be developed each having improved performance. The gas core fission thermal rocket, with a specific power and impulse of ~50 kW/kg and 5000 s, offers the potential for quick courier trips to Mars (of ~80 days) or longer duration exploration/cargo missions (lasting ~280 days) with starting masses of ~1000 metric tons. Convenient transportation to the outer Solar System will require the development of magnetic and inertial fusion rockets (IFRs). Possessing specific powers and impulses of ~100 kW/kg and 200-300 kiloseconds, IFRs will usher in the era of the true Solar System class spaceship. Even Pluto will be accessible with roundtrip times of less than 2 years and starting masses of ~1500 metric tons.					
17. Key Words (Suggested by Author(s)) Nuclear propulsion; Fusion rockets; Solid core; Gas core; NERVA; Nuclear light bulb; Tokamak fusion rocket			18. Distribution Statement Unclassified—Unlimited Subject Category 20		
19. Security Classif. (of this report) Unclassified		20. Security Classif. (of this page) Unclassified		21. No of pages 48	22. Price* A03





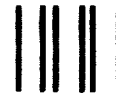
National Aeronautics and  
Space Administration

Lewis Research Center  
Cleveland, Ohio 44135

Official Business  
Penalty for Private Use \$300

FOURTH CLASS MAIL

ADDRESS CORRECTION REQUESTED



Postage and Fees Paid  
National Aeronautics and  
Space Administration  
NASA 451

**NASA**

---